

Pittsburg State University

Pittsburg State University Digital Commons

Electronic Theses & Dissertations

Winter 12-15-2023

ENHANCED MECHANICAL STRENGTH OF SOYBEAN OIL-BASED NON-ISOCYANATE POLYURETHANE ADHESIVE FOR WOOD APPLICATION BY INTRODUCING NANOFILLERS

Vatsal Chaudhari

Pittsburg State University, vchaudhari@gus.pittstate.edu

Follow this and additional works at: <https://digitalcommons.pittstate.edu/etd>

 Part of the [Inorganic Chemistry Commons](#), [Materials Chemistry Commons](#), [Organic Chemistry Commons](#), [Other Chemistry Commons](#), [Physical Chemistry Commons](#), and the [Polymer Chemistry Commons](#)

Recommended Citation

Chaudhari, Vatsal, "ENHANCED MECHANICAL STRENGTH OF SOYBEAN OIL-BASED NON-ISOCYANATE POLYURETHANE ADHESIVE FOR WOOD APPLICATION BY INTRODUCING NANOFILLERS" (2023).

Electronic Theses & Dissertations. 465.

<https://digitalcommons.pittstate.edu/etd/465>

This Thesis is brought to you for free and open access by Pittsburg State University Digital Commons. It has been accepted for inclusion in Electronic Theses & Dissertations by an authorized administrator of Pittsburg State University Digital Commons. For more information, please contact digitalcommons@pittstate.edu.

ENHANCED MECHANICAL STRENGTH OF SOYBEAN OIL-BASED NON-
ISOCYANATE POLYURETHANE ADHESIVE FOR WOOD APPLICATION BY
INTRODUCING NANOFILLERS

A thesis Submitted to the Graduate School
in Partial Fulfilment of the Requirements
For the degree of
Master of Science

Vatsal K. Chaudhari

Pittsburg State University

Pittsburg, Kansas

December 2023

ENHANCED MECHANICAL STRENGTH OF SOYBEAN OIL-BASED NON-
ISOCYANATE POLYURETHANE ADHESIVE FOR WOOD APPLICATION BY
INTRODUCING NANOFILLERS

Vatsal K. Chaudhari

APPROVED:

Thesis Advisor

Dr. Ram K. Gupta, Department of Chemistry

Committee Member

Dr. Khamis Siam, Department of Chemistry

Committee Member

Dr. Timothy Dawsey, National Institute for Materials
Advancement

Committee Member

Dr. John Franklin, Department of English and Modern Languages

Acknowledgments

I would like to express my sincere appreciation to Dr. Ram K. Gupta for becoming the most valuable mentor in my master's journey. Dr. Gupta has played several roles in my academic path, serving as both my instructor and research adviser in the field of polymer chemistry. Furthermore, his continuous support has been invaluable throughout my studies. The unwavering commitment, mentorship, and diligent endeavors of Dr. Gupta have not only served as a source of inspiration but have also provided me with the confidence and drive to actively pursue my ambitions and desires. His profound expertise and wide practical knowledge have successfully facilitated my research endeavors, offering important guidance throughout my academic pursuits at Pittsburg State University (PSU). I have had the opportunity to engage in research work under his guidance, which has greatly enhanced my academic and professional growth.

I would also want to extend my gratitude to Dr. Khamis Siam, Dr. Tim Dawsey, and Dr. John Franklin for serving as members of my thesis committee and providing insightful feedback that helped me conduct my research most beneficially. Along with this, I am thankful to the National Institute of Materials Advancement and the Department of Chemistry, PSU for offering scholarships and financial support. In addition, I would also like to thank Dr. Peter Dvornic, Mr. Paul Herring, and Dr. Jeanne Norton for providing me with good hands-on polymer chemistry. The support of my labmates and friends, Arjun, Sahil, Akshay, Nirmal, Vishwa, Rishabh, Himanshu, Sagar, Yash, Jainish, Uday, and Sahithi made my academic journey pleasurable and unforgettable at PSU.

Ultimately, my father Mr. K.L Chaudhari, and my Mother Mrs. Sharadaben Chaudhari deserve the deepest appreciation who loved me selflessly and supported me in every stage of my life and are my biggest source of motivation. My parents provided me

with emotional and financial support during my entire educational journey. I would also like to express my gratitude to all individuals who helped throughout my master's program.

ENHANCED MECHANICAL STRENGTH OF SOYBEAN OIL-BASED NON-ISOCYANATE POLYURETHANE ADHESIVE FOR WOOD APPLICATION BY INTRODUCING NANOFILLERS

An Abstract of the Thesis by
Vatsal K. Chaudhari

Polyurethane (PU) is a versatile material that finds extensive use in various industries including bedding, construction, automotive, and packaging. Historically, this particular polymer relied significantly on petrochemical resources, a practice that was considered to have negative environmental impacts. The conventional method for preparing PU involves the use of isocyanate, which is a disadvantage due to its negative impact on the environment and human health. The resolution of this problem entails identifying an appropriate substitute for petroleum-derived products that minimize their impact on both the environment and human health. Researchers earlier utilized soybean oil for the formulation of PUs in this replacement [1]. Hence, researchers are consistently conducting experiments on non-isocyanate polyurethane (NIPU).

This study focuses on the preparation of non-isocyanate polyurethane for use as a wood adhesive. The process involved epoxidation, followed by carbonation, to produce carbonated soybean oil. The synthesized carbonated soybean oil (CSBO) was then blended with ethylenediamine (EDA) to produce a NIPU adhesive network. To analyze the synthesized CSBO, various confirmatory tests such as Fourier transform infrared spectroscopy (FT-IR), gel permeation chromatography (GPC), viscosity, iodine value, and epoxy value were conducted. The synthesized NIPU adhesive was characterized using thermogravimetric analysis (TGA) and differential scanning calorimetry (DSC). Furthermore, to investigate improvements in the thermal and mechanical characteristics of

the green polyurethane glue, silicon (Si) nanoparticles were included as a filler, with different particle sizes of about 100 nm, 200-300 nm, and 500 nm. In addition, to investigate the tensile strength of the NIPU adhesive, a single lap joint specimen was subjected to testing using a tensile testing instrument. To cure the specimen, a manual clamping technique was used, and specimens were then kept in the oven at various temperatures and times to achieve the ideal sample for further testing with fillers. With the control NIPU sample, 8.81 MPa of shear strength was recorded. As expected, after incorporating fillers in NIPU adhesive, the highest shear strength was achieved at 9.85 MPa. Apart from this, a contact angle test was also performed to observe the hydrophobicity of the sample. This work brought a facile path to produce NIPU adhesive from soybean oil which could be further used as a wood adhesive.

TABLE OF CONTENTS

CHAPTER I	1
INTRODUCTION.....	1
1.1. Chemistry of polyurethanes.....	1
1.2. Applications of polyurethanes	3
1.3. Types of polyurethanes	4
1.4. Soybean oil	5
1.5. Wood.....	6
1.6. Adhesion	7
1.6.1 Wood adhesion.....	7
1.7. Adhesive	8
1.8. Research objective.....	9
CHAPTER II.....	11
MATERIALS AND METHODS	11
2.1 Materials	11
2.1.1. Soybean oil.....	11
2.1.2. Ethylenediamine	12
2.1.3. Fillers	13
2.1.4. Si nanoparticles (100, 200-300, and 500 nm).....	13
2.2. Synthesis of CSBO	14
2.2.1. Epoxidation of soybean oil	14
2.2.2. Carbonation of ESBO	16
2.2.3. Synthesis of NIPU samples.....	17
2.3. Adhesive preparation	18
2.4. Characterization of CSBO	19
2.4.1. Iodine value.....	19
2.4.2. Epoxy value	19
2.4.3. Fourier-transform infrared spectroscopy	20
2.4.4. Gel permeation chromatography (GPC).....	20
2.4.5 Viscosity.....	21
2.5. Characterization of NIPU adhesive	22
2.5.1. Thermogravimetric analysis (TGA).....	22
2.5.2. Differential scanning calorimetry analysis (DSC).....	23
2.5.3. Shear strength measurement	24
2.5.4. Water Contact Angle	25
CHAPTER III	27
RESULTS AND DISCUSSION	27
3.1. Synthesis of ESBO & CSBO.....	27
3.1.1. Iodine value.....	27
3.1.2. Epoxy value	27
3.1.3. Fourier-transform infrared spectroscopy	28
3.1.4. Gel permeation chromatography.....	29
3.1.5. Viscosity.....	30
3.2. TGA.....	31

3.3. DSC	37
3.4. Contact angle measurement.....	41
3.5. Single-lap shear strength	42
3.5.1. Control sample.....	45
3.5.2. Effect of the Si nanofillers	46
CHAPTER IV.....	54
CONCLUSION.....	54
CHAPTER V	56
FUTURE WORK	56
REFERENCES:	57

LIST OF TABLES

Table 1: TGA data for weight loss.....	37
Table 2: Locus of failure in NIPU adhesive.....	50
Table 3: Comparison with other PU adhesives.....	53

LIST OF FIGURES

Figure 1: Reaction between diisocyanate and polyol.....	2
Figure 2: Types of polyurethanes with their applications.....	4
Figure 3: Chemical structure of soybean oil.....	12
Figure 4: Chemical structure of EDA.....	12
Figure 5: Epoxidation and carbonation reaction of soybean oil.....	17
Figure 6: Digital photo of the FT-IR instrument used in this research.....	20
Figure 7: GPC instrument used in this research.....	21
Figure 8: Digital image of the viscosity instrument used in this research.....	22
Figure 9: Digital photo of the TGA analysis instrument used in this research.....	23
Figure 10: Digital photo of the DSC instrument used in this research.....	24
Figure 11: Digital image of the lap shear strength instrument used in this research.....	25
Figure 12: Digital image of the contact angle instrument used in this research.....	26
Figure 13: FTIR analysis of SBO, ESBO, CSBO, and NIPU.....	29
Figure 14: GPC analysis of SBO, ESBO, and CSBO.....	30
Figure 15: TGA analysis results.....	33,34,35,36
Figure 16: DSC plot of samples with (a) Variation in curing time (b) Si 100 nm (c) Si 200-300 nm (d) Si 500 nm	39,40
Figure 17: Contact angle of the control sample, Si 100, 200~300, and 500 nm nanofillers samples.....	42
Figure 18: Dimensions of oak wood.....	43
Figure 19: Manual clamping method.....	44
Figure 20: Tensile test performed on Instron M 3367.....	44
Figure 21: Substrate failure observed in specimens.....	45
Figure 22: Shear strength with variation in curing times and temperatures.....	46
Figure 23, 24, &25: Shear strength of NIPU adhesives varying Si nanoparticles...47,49	

LIST OF ABBREVIATIONS

PU	Polyurethane
NIPU	Non-isocyanate polyurethane
ESBO	Epoxidized soybean oil
CSBO	Carbonated soybean oil
EDA	Ethylenediamine
FTIR	Fourier transform infrared spectroscopy
GPC	Gel permeation chromatography
DSC	Differential scanning calorimetry
TGA	Thermogravimetric analysis
CASE	Coatings, Adhesives, Sealants, And Elastomers
Si	Silicon
TDI	Toluene diisocyanate
MDI	Methylene diphenyl diisocyanate
CMR	Carcinogenic, Mutagenic, and Reprotoxic

CHAPTER I

INTRODUCTION

1.1. Chemistry of polyurethanes

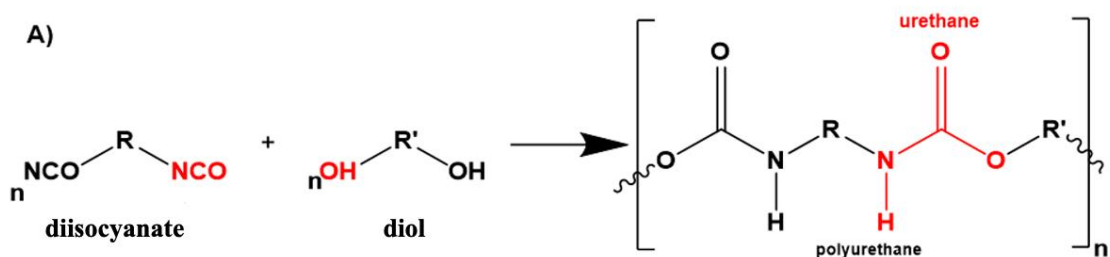
Polyurethanes (PUs) are polymeric materials that have repeating urethane linkage $[\text{NH}-\text{C}(\text{O})-\text{O}]$ [2]. PU is considered a highly versatile polymer due to its ability to be synthesized using a diverse range of starting materials. Due to their capacity to meet demands ranging from physical behavior to chemical properties, from innovative applications to sustainability, PUs are essential in a wide range of sectors. The first PU was developed by Otto Bayer and collaborators in 1937, through the reaction of diol and diisocyanate from a polycondensation reaction [3]. In 1952, after undergoing certain improvements, it was possible to achieve an industrial manufacturing scale. The advances in polyurethane technology and the incorporation of polyurethane into daily life have raised the standard of living globally.

PU has found widespread application in the adhesive, paint, flexible/rigid foams, biomedical, automotive, and aerospace sectors, amongst other applications [4]. The versatility of PU can be understood from the fact that it is employed both in thermosets and thermoplastic forms in industry [5]. With a global market of 67.13 billion USD in 2022 and estimated to reach 105.2 billion USD by 2025, PU was the sixth most produced polymer in the world [6]. PUs may be acquired using simple methods that involve a polyaddition

reaction between a precursor material having multiple hydroxyl groups, such as diol or polyol (–OH), and a polyisocyanate (–NCO), resulting in the formation of a urethane bond as shown in **Figure 1** [7].

Figure 2: Reaction between diisocyanate and polyol

Traditionally, PUs have been produced using components derived from petrochemical sources like crude oil. The excessive use of non-renewable resources employed for the



manufacturing of PUs combined with extremely toxic and volatile isocyanates such as toluene diisocyanate (TDI) and methylene diphenyl diisocyanate (MDI) which are classified as CMR (Carcinogenic, Mutagenic and Reprotoxic) has proved hazardous to the environment and human health [8], [9]. Another reason is that the production of isocyanate involves the phosgene gas which is known to be very toxic and harmful [4]. Because of this, it is essential to develop innovative strategies that will reduce negative environmental effects while making use of commercially viable components without compromising the qualities of the polymer [10]. To resolve these concerns, scientists and researchers over the past few years have focused on finding a suitable alternative to petroleum-based PUs which has been raising environmental concerns over the years. Preparing a synthesis procedure through a non-isocyanate route can be considered a novel approach.

To overcome these challenges, significant progress has been made in the production of polyols from bio-renewable sources, including rapeseed oil [11], canola oil [12], sunflower oil [13], corn oil [14], soybean oil [15] and other examples found throughout the literature [16], [17]. As a result, a new age of non-isocyanate-based PU (NIPU) came into the limelight. NIPU can be prepared by reacting cyclic carbonates with amines [1].

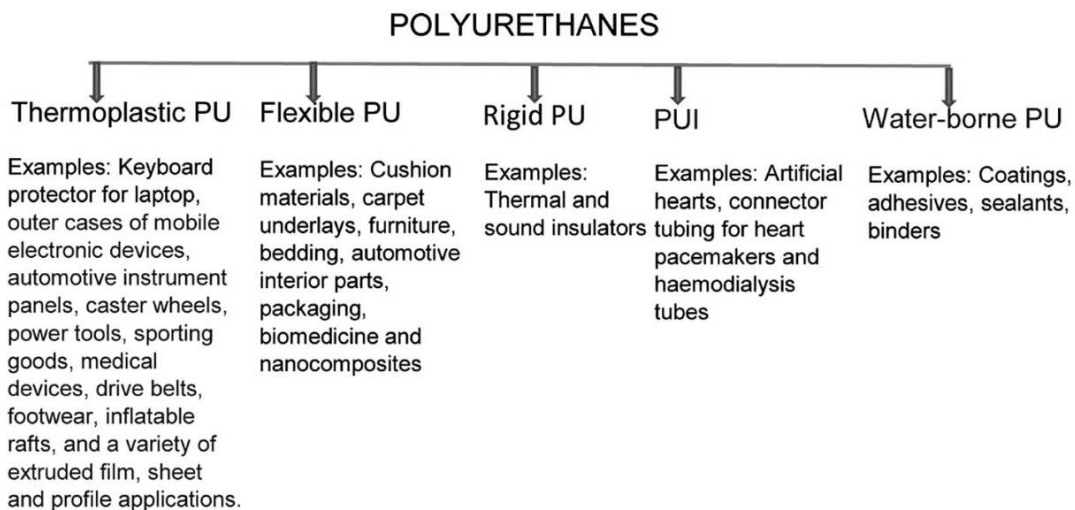
1.2. Applications of polyurethanes

PU are a highly notable category of industrial polymers that currently hold a prominent position in the global market, experiencing rapid growth. Outstanding chemical resistance, durability, and toughness are some of the key advantages of the PUs. PUs are extensively used in various fields of polymer applications, including but not limited to foams, elastomers, thermoplastics, thermosetting materials, adhesives, coatings, sealants, and fibers. Currently, PUs possess a substantial portion of the plastic industry's market share, particularly in the field of coatings, adhesives, sealants, and elastomers (CASE) [18]. Other than CASE industries, PUs have a huge range of applications in the aerospace, automotive, and biomedical sectors. PUs recorded an annual global production of 18 metric tons in 2016 [4] which makes this compatible and one of the most used polymers. Despite being a firmly established industry, the extensive utilization of non-renewable resources in the production of PUs has resulted in increasing environmental concerns over time. To resolve this concern, researchers are investigating innovative approaches without affecting the properties of the polymer. Due to their enormous properties, PUs have been utilized in a variety of commercial applications.

1.3. Types of polyurethanes

There are various varieties of polyurethanes based on their synthesized pathway, chemical structure, and applications. There are five types of PUs displayed in **Figure 2** that are utilized on a global scale, which are as follows: rigid PU, flexible PU, thermoplastic PU, polyurethane ionomers (PUI), and waterborne PU (WBPU). Rigid PU is mostly produced to make foams and is widely acknowledged for its versatility and energy-efficient capabilities as an insulation materials. On the one hand, these foams possess the inherent capacity to significantly reduce energy expenditures, while on the other hand, they exhibit the capability to improve the comfort and efficacy of both commercial and residential appliances [19]. Thermal and sound insulators are some of the best examples.

Figure 2: Types of polyurethanes with their applications. Adopted with permission [19], Copyright 2016, Royal Society of Chemistry



Flexible polyurethane (FPU) foams consist of block copolymers that exhibit flexibility because of the soft and hard segments' phase separations [20]. Flexible PUs may be categorized according to certain physical features, such as density, toughness, tearing

resistance, combustibility, surface elasticity, etc., wherein an array of these qualities may ensure good flexibility in the PU compound [19]. Flexible PU foams are extensively utilized as cushion materials in various commercial applications encompassing bedding, furniture, car seats, packaging, and nanocomposites [19]. Thermoplastic polyurethanes (TPUs) exhibit a wide range of physical characteristics and find extensive utility in many processing applications. Generally, TPUs reveals an elastic and flexible nature with excellent abrasion resistance property. This is due to the combination of soft and hard segments in the PU which led to the stretching of a material without any deformation for a longer period and makes this PU ideal for different applications. TPUs have good thermal stability until 235 °C [21]. Mobile cases, electronic devices, keyboard protectors, footwear, medical devices, and sporting goods are some of the examples of TPUs applications.

PUI is mostly utilized in biomedical devices due to its biocompatibility and shape memory features. The composition of soft and hard segments within PU molecules, as well as their molecular arrangement, exert an influence on the shape memory effect (SME) of the PU material which makes them the best choice for biomedical applications. It is applied in making artificial hearts, haemodialysis tubes, and connector tubing for heart pacemakers [22]. Coatings and adhesives that rely largely on water as the solvent are typically referred to as waterborne polyurethanes.

1.4. Soybean oil

Soybean oil is a pale-yellow color oil obtained from the seeds of glycine max, also known as soybean [23]. The cultivation of soybeans in China can be traced back to approximately 4000-5000 years ago. Following the year 1954, the United States of America emerged as the global leader in the domain of soybean production and subsequent

exports. The composition of soybean oil is comprised of saturated, monounsaturated, and polyunsaturated fats. Soybean oil is characterized by a substantial quantity of unsaturated fatty acids, primarily in the form of triglycerides. The composition of this substance includes polyunsaturated-linoleic acid, which accounts for 51% of its content, as well as alpha-linoleic acid, present at a range of 7-10%. Additionally, monosaturated-oleic acid makes up approximately 23% of the composition.

Soybean oil has a distinct fatty acid content (FAC) that is generally resistant to environmental influences [24]. The processing of soybean oil involves three primary stages: initial preprocessing, following extraction and separation, and final postprocessing [24].

1.5. Wood

Wood consists primarily of two chemical constituents: carbohydrates, comprising 65-75% of its composition; and lignin, accounting for 18-35% and elemental composition of carbon (50%), oxygen (44%), and hydrogen (6%) with some trace of metal ions [25]. Carbohydrates contain cellulose and hemicellulose, ranging from 40–50% and 25–35%, respectively [25]. Due to its significant characteristics and great practical applications, wood is a widely utilized material. Construction, furniture, instruments, and packaging are some of the best examples of wood application. In this research work, oak wood was utilized to prepare and test the specimens.

1.6. Adhesion

In simple terms, when different molecules or surfaces bind together then the process is known as adhesion. Adhesion can be categorized into different types such as mechanical interlocking, chemical bonding, and physical bonding [26]. The phenomenon of mechanical interlocking clarifies the adhesive's tendency to disperse or spread across the surface and establish wetting on the substrate's surface by interlocking mechanically. Velcro closure is one of the suitable examples of mechanical interlocking [26]. The process of chemical bonding includes the formation of a covalent bond between the adhesive and the surface of the substrate. Ionic and chelation bonding are present in some cases. Physical bonding refers to the occurrence of Van der Waals forces and hydrogen bonding during the interaction between surface and adhesive. In addition to these theories, diffusion and electron transfer are the other two accepted theories on adhesion [27].

1.6.1 Wood adhesion

The process of binding wood surfaces by applying adhesive to build a robust bonding is known as wood adhesion. There are various requirements to prepare an effective wood adhesion such as surface roughness, wetting, curing, proper contact angle, and low viscosity of adhesives with an adequate flow. To achieve an effective wetting, the contact angle between the surface and the edge of the droplet of adhesive should be minimized/low because wetting is one of the key reasons for getting excellent bonding strength. Along with wetting, the flow of the adhesive across the surface is also required for the formation of strong bonding. Curing is also one of the significant requirements that comes after wetting the surface. Curing is the process where a liquid state is converted into a solid state.

Various curing techniques such as heat curing, UV curing, hot press, and moisture curing are applied to solidify the adhesive for further application.

1.7. Adhesive

An adhesive is a non-metallic material that is applied to one or both surfaces of two different objects to bind them together and prevent them from being separated. About 2000 BC, the traces of adhesives were first mentioned in literature. Adhesives offer a huge variety of applications in various fields like packaging, furniture, aerospace, automotive, manufacturing carpets, security tapes, and binding paper. An adhesive can be prepared both naturally and synthetically. Synthetic resin-based adhesives are generally prepared using petroleum-based products. Prior to World War II, wood adhesives were produced using natural materials like mud and clay. However, due to the strong bonding strength quality, synthetic resin-based adhesives became very popular and widely used adhesives after World War II.

Generally, synthetic resin-based wood adhesives fall into two categories: thermosetting and thermoplastic adhesives. Thermosetting adhesives exhibit irreversible reaction due to the formation of the chemical bond and cross-linking when it is cured and converts them into a permanent shape that cannot be recycled. On the other hand, thermoplastic adhesives exhibit reversible reactions and they do not form chemical bonds or cross-linking when cured which makes them recyclable. PU, Epoxy, Urea-formaldehyde (UF), phenol resorcinol formaldehyde (PRF), phenol-formaldehyde (PF), melamine-formaldehyde (MF), melamine urea formaldehyde (MUF), and resorcinol formaldehyde (RF) are the examples of thermosetting adhesives. PU adhesives show good flexibility at

low temperatures, impact resistance, and durability [28]. Epoxy adhesives are easy to use and have low cost with high strength [28]. The use of UF-based adhesives is restricted to applications involving interior plywood and particleboard. PF is water-repellent, has a low viscosity, and is temperature stable [29]. A significant amount of MF adhesive is utilized in the production of adhesive for external and semi-exterior wood panels. Polyvinyl acetate (PVA) and polyamide (PA) are two commonly used thermoplastic adhesives.

Formaldehyde holds a prominent position in the majority of the wood adhesive market. But formaldehyde-based adhesives are produced from non-renewable sources and are also toxic in nature which has raised environmental concerns over the years. The production process relies on the oil industries which can lead to price hikes. To overcome these concerns, researchers are trying to find a suitable replacement for formaldehyde-based adhesives. Bio-based adhesives have gained significant attention among scientists and researchers. Polyol which is a starting material to make adhesives can be prepared from various vegetable oils like soybean oil, sunflower oil, and canola oil.

1.8. Research objective

The purpose of this research work is to utilize soybean oil as a suitable alternative to petroleum-based wood adhesives. In this study, NIPU was prepared for the application of wood adhesive. Epoxidation was performed, followed by carbonation to produce CSBO. Confirmatory tests such as FT-IR, iodine value, epoxy value, GPC, and viscosity were conducted to identify the formation of CSBO and PU. The fundamental objective of this research was to observe the effect of the particle size of silicon (Si) filler on the shear strength of the wood adhesive. Three Si nanoparticle sizes (100, 200-300, and 500 nm)

were introduced to determine the effect of nanofillers on the thermal properties of the NIPU adhesive synthesized from soybean oil.

CHAPTER II

MATERIALS AND METHODS

2.1 Materials

2.1.1. Soybean oil

Soybean oil is derived from the seeds of glycine max(soybean) [23]. Soybean oil has a composition of saturated, monosaturated, and polyunsaturated fats. Triglycerides – a large amount of unsaturated fatty acids is present in soybean oil. This contains polyunsaturated-linoleic acid (51%) and alpha-linoleic acid (7-10%); and monosaturated-oleic acid (23%). The C=C seen in the triglycerides of soybean oil served as the primary focus of this work's efforts to generate additional reactive sites during further synthesis. The soybean oil used in this experiment was purchased from a local Walmart (Pittsburg, KS, USA) and employed without additional purification. The viscosity of soybean oil was found to be 0.19 Pa.s at room temperature. **Figure 3** displays the chemical structure of soybean oil. The central objective of this study was to enhance the reactivity of soybean oil's carbon-carbon double bond within triglycerides, to generate supplementary reactive sites during further synthesis. Herein, soybean oil was used as a starting material for the synthesis of bio-based PU wood adhesive.

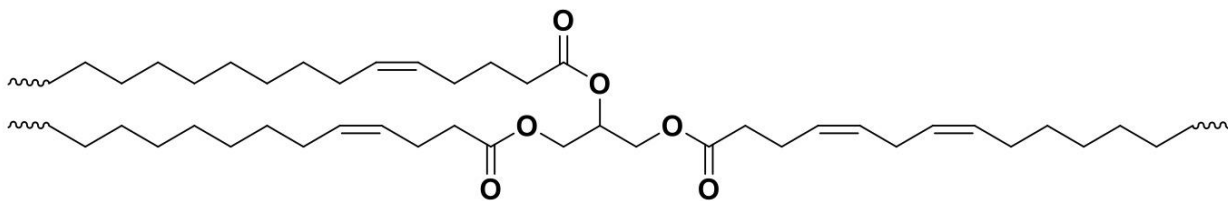


Figure 3: Chemical structure of soybean oil

2.1.2. Ethylenediamine

EDA is an organic compound having a structural formula $C_2H_4(NH_2)_2$. EDA is classified as a diamine, which is a class of chemical compounds that are distinguished by the presence of two amino groups ($-NH_2$) and are partitioned from one another by an ethylene chain ($-CH_2CH_2-$). It is manufactured on an industrial scale by reacting 1,2-dichloroethane with ammonia (NH_3). It plays a crucial role in the preparation of polyurethane. In the formation of adhesive, it functions as a cross-linker. In this research work, EDA was purchased from Acros Organics, (NJ, USA). The chemical structure of EDA is shown in **Figure 4**.

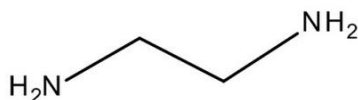


Figure 4: Chemical structure of EDA

2.1.3. Fillers

To improve the thermal and mechanical properties of PU adhesive, various nanofillers are incorporated into their composition. Introducing fillers can reduce costs along with enhancing the mechanical properties of the PU adhesives [30]. To observe the effect of particle size of nanofiller on the bonding strength of the adhesive, Si nanoparticles (99%, 100 nm), monocrystalline Si nanoparticles (99%, 200-300 nm), and Si nanoparticles (99%, 500 nm) were introduced to observe the increment in mechanical and thermal properties.

2.1.4. Si nanoparticles (100, 200-300, and 500 nm)

Si nanoparticles are composed of Si, a chemical element renowned for its natural occurrence and significant contributions to advanced technology. Si was discovered by a well-known scientist Jons Jacob Berzelius in 1823. The mechanical characteristics of PU adhesives are profoundly affected by the particle size of nanofillers. Si is one of the most abundant materials found on the earth. To produce Si with a purity of 96 - 99%, quartzite or sand must be carbothermally reduced with highly pure coke. Si as a filler, contributes to the prevention of excessive penetration into the wood specimen. The primary focus of this work is to enhance the bonding strength by adding three different particle sizes of Si (100, ~250, and 500 nm) as a filler.

Si nanoparticles 100 nm appear as a yellow-brown powder that is composed of spherical particles of Si with an average particle size of 100 nm. It contains 99% pure Si and <45% copper (Cu). Two common parameters for 100 nm are surface area: >80 (m²/g) and density: 0.08 (g/cm³) for Si 100 nm. Si nanoparticles ~250 nm are monocrystalline in

nature with a melting point (m.p) of 1414°C and boiling point (b.p) of 2900°C. It exhibits a dark grey appearance. Purity: 99.9%; M.P: 1414°C; B.P: 2900°C are some frequently encountered parameters for Si 500 nm particle size. Si nanoparticles (100, ~250, and 500 nm) were purchased from SkySpring Nanomaterials, Inc. (TX, USA).

2.2. Synthesis of CSBO

In order to produce bio-based CSBO from soybean oil, a two-step process called epoxidation followed by carbonation was carried out.

2.2.1. Epoxidation of soybean oil

Epoxidation refers to the chemical transformation wherein an oxygen bridge is introduced across a double bond, resulting in the formation of an epoxide. Epoxide groups have a high level of reactivity, which makes them useful as active intermediates in the production of chemicals that are important to the economy. These compounds include alcohols, glycols, alkaloamines, carbonyl compounds, and olefinic compounds, as well as polymers such as polyester, polyurethane, and epoxy resin [31]. There are four possible methodologies for the synthesis of epoxies derived from alkene(C=C). These methodologies encompass the process of epoxidation utilizing percarboxylic acid, both organic and inorganic peroxides, and halohydrins, as well as molecular oxygen.

Acetic acid functioned as an agent for oxygen donation, whereas hydrogen peroxide functioned as a facilitator for oxygen transportation. Hence, an epoxide ring was converted by the double bond of oil [32]. The molar ratio of the double bond to acetic acid to hydrogen peroxide in the epoxidation process of soybean oil was 1:0.5:1.5. In the first step, a three-

necked round-bottom flask was used to combine 300 g of soybean oil (SBO) and 150 mL of toluene, which had a weight percentage of 50% SBO. Subsequently, a quantity of 75 g of Amberlight IR 120H resin, serving as the catalyst, was introduced. The solution was agitated for a duration of 15 minutes in order to attain a uniform and consistent mixture. Subsequently, a total volume of 43.9 mL of acetic acid was incrementally introduced into the system through the utilization of a dropping funnel. The solution was subsequently agitated for a duration of 30 minutes.

A volume of 180 mL of a hydrogen peroxide solution with a weight percentage of 30% was incrementally introduced into the mixture, maintaining the temperature within the range of 5 to 10 °C. Following the full addition of hydrogen peroxide, the temperature was raised and sustained at 70 °C for a duration of 7 hours. The aforementioned experimental protocol was executed to synthesize peracetic acid in situ through the chemical reaction between acetic acid and hydrogen peroxide. In this context, it is plausible for peracetic acid to undergo a chemical reaction with the double bonds present in the chemical structure of SBO, resulting in the formation of an epoxy group at position 35. The mixture was subjected to a cooling process and subsequently underwent filtration to isolate the resin. The mixture then underwent a series of washes employing a 10% brine solution until a neutral pH of 7 was attained. The yield of epoxide soybean oil ESBO was determined to be approximately 80%. After the successful synthesis of ESBO, a series of confirmatory tests were conducted, including Fourier Transform Infrared Spectroscopy (FT-IR), epoxy number determination, and Gel Permeation Chromatography (GPC) analysis.

2.2.2. Carbonation of ESBO

The utilization of ESBO, also a commercially available substance, serves as the initial reactant that undergoes a chemical reaction with carbon dioxide in the presence of the TBAB catalyst, resulting in the formation of CSBO [33]. This process is known as carbonation.

The reaction was performed under the controlled temperature and pressure in the Parr reactor. In the beginning, a total of 300 grams of ESBO and 0.05 moles of TBAB catalyst per mole of epoxy groups were carefully introduced into a 500 mL Parr reactor, while maintaining a CO₂ pressure of 3.79 MPa (550 psi). The reaction was carried out for a duration of 48 hours at a temperature of 110 °C while maintaining a stirring speed of 1100 rpm. Upon completion of the reaction, the epoxy oxygen content (EOC) was approximately 0.20%, indicating a successful carbonation process. A remarkable conversion rate of 94.3% was attained in the transformation of epoxy groups into cyclic carbonate groups. **Figure 5** illustrates a schematic displaying the reactions of the epoxidation and carbonation of soybean oil.

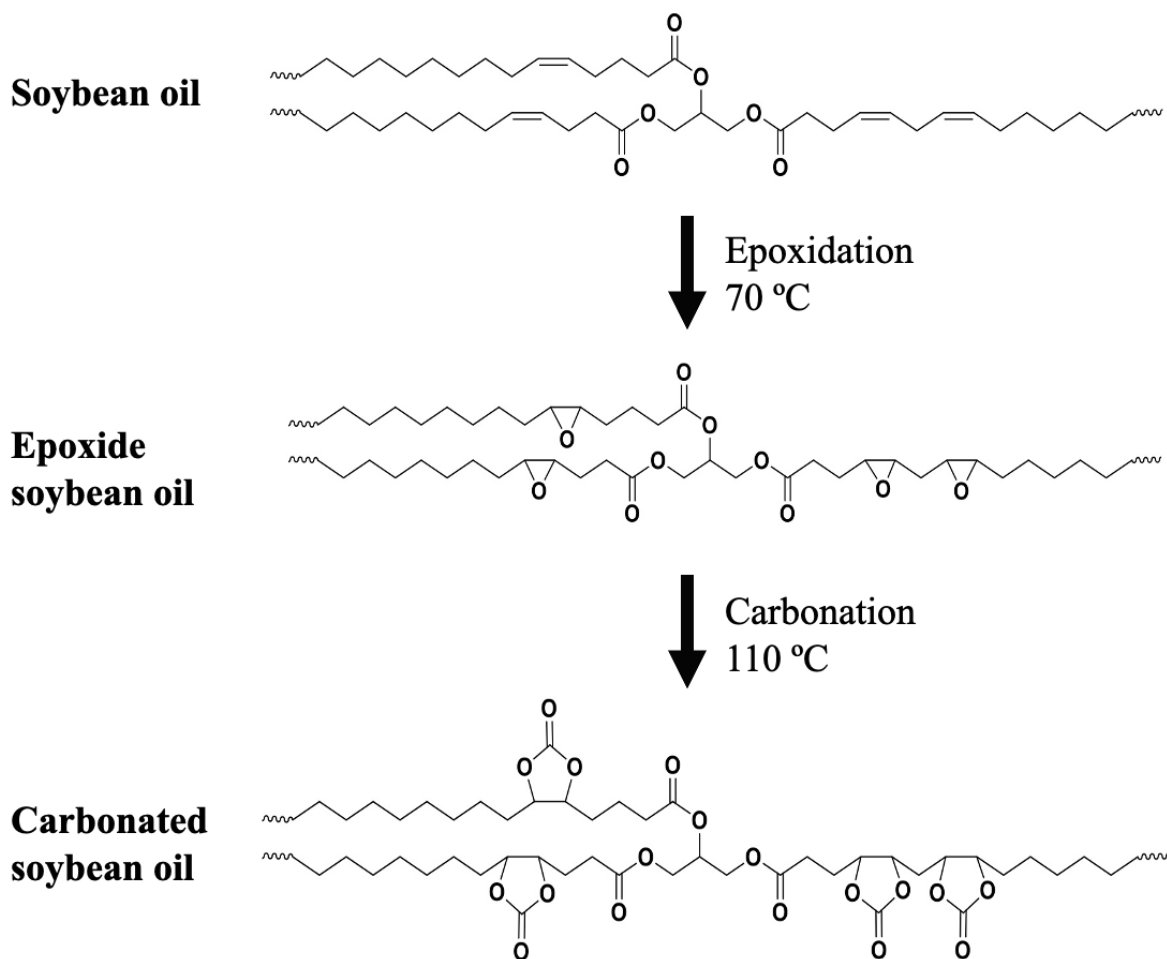


Figure 5: Epoxidation and carbonation reaction of soybean oil

2.2.3. Synthesis of NIPU samples

In the process of synthesizing NIPU wood adhesive, it was observed that the reactants, namely CSBO and EDA, underwent a chemical reaction in a stoichiometric molar ratio of 1:1. In the experimental setup, a total mass of 3.5 grams of CSBO was introduced into a beaker as the initial step. Subsequently, a mass of 0.73 grams of EDA was meticulously added drop by drop. Following the addition of EDA, the mixture underwent

stirring for 1 minute utilizing a spatula, thereby facilitating the homogenization of the system. By executing this process, the control sample for the NIPU adhesive was acquired.

2.3. Adhesive preparation

A study was conducted to investigate the curing process of the NIPU adhesive, which was synthesized. The NIPU adhesive was applied to a 25 mm × 25 mm (length × width) oak board. Then, various curing procedures were carried out at different temperatures 60, 80, 100, and 120°C, respectively, and variation in time 30, 60, 90, and 120 minutes, respectively. A study was undertaken to determine the most effective curing condition for enhancing the shear strength of the NIPU adhesive. Based on the aforementioned observations, it was found that subjecting NIPU to a temperature of 80 °C for 90 minutes resulted in the most favorable outcomes. These results will be elaborated further.

Once the appropriate curing conditions were established, a batch of NIPU adhesives was produced using the same methodology. However, in this case, various amounts of Si nanoparticles with a specified size were incorporated into the adhesives. The ideal curing process, consisting of subjecting the adhesives to a temperature of 80 °C for a duration of 90 minutes, was then applied. In this research, we incorporated Si nanoparticles with varying weight percentages (1, 3, 5, 7, 10, and 15 wt.%) and average sizes (100, 250, and 500 nm) into individual samples of NIPU adhesive.

2.4. Characterization of CSBO

2.4.1. Iodine value

The determination of the iodine content of soybean oil was one of the most important and preliminary experiments conducted as part of this research. The iodine number is a quantitative measure that can be employed to ascertain the quantity of double bonds within an unsaturated compound. Iodine can successfully react with a double or triple bond that is present in an unsaturated substance. A higher iodine value signifies that the fatty acid exhibits increased reactivity and decreased stability[34]. The number of iodide ions that are attached to the unsaturated carbon chain can be determined by the iodine value[34]. The Hanus titration method was employed in this experiment to estimate the number of double bonds in soybean oil utilized in the preparation of CSBO.

2.4.2. Epoxy value

In order to ascertain the epoxy oxygen content (EOC %), a combination of glacial acetic acid and tetraethylammonium bromide was employed. With this method, the examination and verification of the formation of epoxide groups from double bonds was carried out. Epoxidized soybean oil (0.3 g) was diluted in tetraethylammonium bromide (TEAB) solution (50 mL) for this analysis. After adding a drop of crystal violet indicator, the solution was titrated with 0.1 N perchloric acid (HClO₄). When a color change from blue to green was observed, titration ended. The obtained volume was further utilized for the determination of the amount of epoxy present in the ESBO. An average of 3 tests was calculated.

2.4.3. Fourier-transform infrared spectroscopy

The Fourier transform infrared spectroscopy (FT-IR) technique is a successful approach for determining the presence of a variety of functional groups in the material. The FTIR spectrometer has the ability to acquire spectral data with high resolution across a broad range of wavelengths simultaneously. The PerkinElmer Spectrum Two FT-IR Spectrophotometer (**Figure 6**) was employed to acquire spectral data of synthesized materials under normal temperature conditions in order to evaluate the organic components contained within the chemical structure [7].



Figure 6: Digital photo of FT-IR instrument used in this research

2.4.4. Gel permeation chromatography (GPC)

GPC is also called size exclusion chromatography in which analytes are segregated based on their molecular weight (size), typically within the confines of organic solvents. Determination of the retention time is a significant factor in GPC because it confirms the successful conversion of the synthesized material. Retention time is directly correlated to

molecular weight as the higher the retention time, the lower the molecular weight of the material. This method is commonly used for the analysis of polymers. After conducting the epoxidation and carbonation processes, a characterization approach was utilized to confirm the ESBO and carbonated soybean oil CSBO from the oil. In this work, The Waters GPC instrument from Milford, MA, USA was utilized and shown in **Figure 7**. Moreover, THF was used as the solvent with a flow rate of 1mL/min at 30 °C.

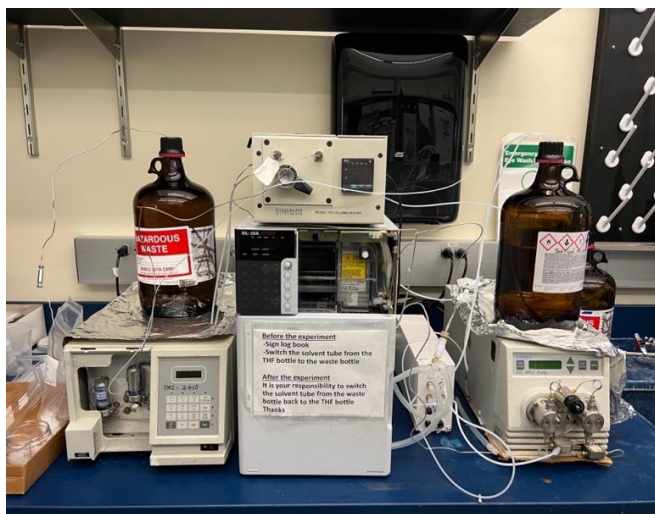


Figure 7: GPC instrument used in this research

2.4.5 Viscosity

Viscosity is a measurement of the level of resistance experienced by a material during its flow. Significant insights can be derived from various factors, including intermolecular interactions, molecular weight, and the progression of reactions, among other important components. Viscosity is also directly proportional to the molecular weight of a material. High viscosity indicates that molecular weight is also high, whereas low viscosity signifies low molecular weight. An AR 2000 dynamic stress rheometer (TA

Instruments, USA) was used as displayed in **Figure 8**. The viscosity was determined at a temperature of 25 °C, where the shear stress was progressively increased from 1 to 200 Pa. The dynamic rheometer was installed with a cone plate that had an angle of 2° and a cone diameter of 25 mm.



Figure 8: Digital image of the viscosity instrument used in this research

2.5. Characterization of NIPU adhesive

2.5.1. Thermogravimetric analysis (TGA)

To determine the thermal stability of NIPU adhesives with variations in filler size and various curing times, samples were analyzed through the TGA (Q500, Discovery, Trios, USA) instrument as displayed in **Figure 9**. The thermal decomposition of samples was performed under nitrogen flow at a ramp rate of 10° C/min and a temperature range of 25–600 ° C.

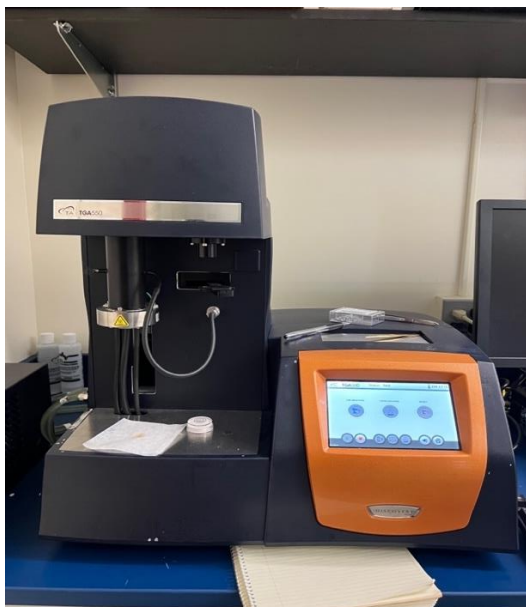


Figure 9: Digital photo of the TGA analysis instrument used in this research

2.5.2. Differential Scanning Calorimetry analysis (DSC)

The thermal transition temperature of the NIPU was characterized by the analysis of DSC to observe variations in the physical characteristics of specimens and their temperature over time. This instrument is mainly utilized to measure glass transition temperatures (T_g), melting temperature (T_m), and crystallization temperature (T_c). As shown in **Figure 10**, all of the DSC tests that were performed for this study were carried out with the DSC Q100 instrument (TA Instruments, USA). All the tests were performed in the temperature range of -70 to 260°C with a $10^\circ\text{C}/\text{min}$ ramp rate.

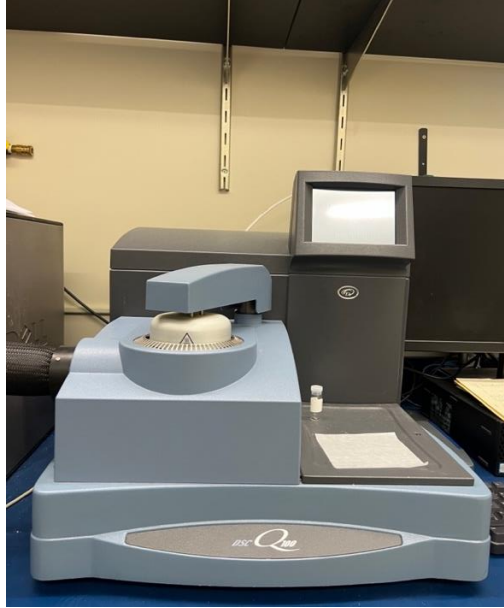


Figure 10: Digital photo of the DSC instrument used in this research

2.5.3. Shear strength measurement

To determine the bonding strength of the substrate, NIPU adhesive was applied on the oak wood substrate, and a single-lap dry shear strength test was carried out using an Instron Model 3367 (Instron, USA) as illustrated in **Figure 11** with a 10 mm/min crosshead speed. Oak wood with an application area of 25 mm × 25 mm (length × width) was used to perform tests. Shear strength was measured according to the ASTM Standard Procedure D2339-98. An average of three specimens was recorded under the maximum load.



Figure 11: Digital image of the lap shear strength instrument used in this research

2.5.4. Water Contact Angle

To examine the surface morphology of the NIPU adhesive, a water contact angle measurement was carried out utilizing an Ossila Contact Angle Goniometer as shown in **Figure 12**. To obtain hydrophobicity on the wood specimen, the adhesive was applied smoothly throughout its surface. To conduct this test, 10 μL of HPLC-grade water droplet was measured and deposited on the surface of the specimen at room temperature.

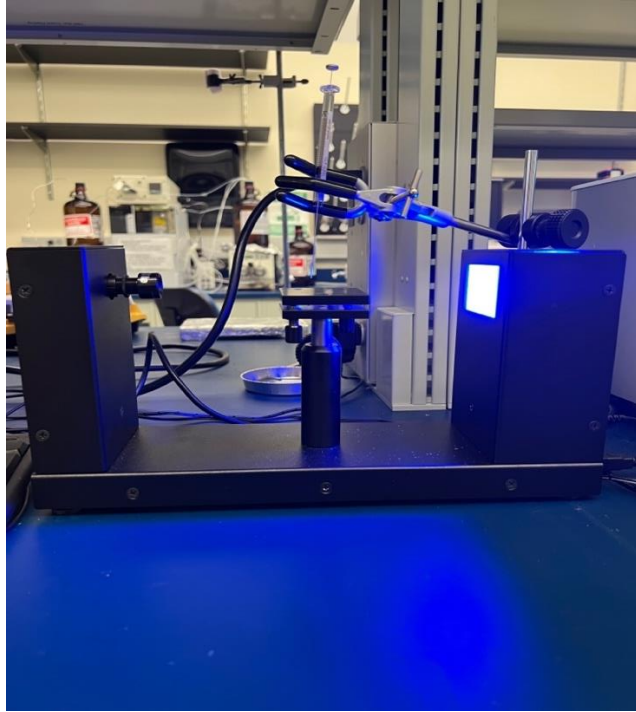


Figure 12: Digital image of contact angle instrument used in this research

CHAPTER III

RESULTS AND DISCUSSION

3.1. Synthesis of ESBO & CSBO

3.1.1. Iodine value

Iodine value evaluates the degree of unsaturation or the quantity of double bonds in oil. Hanus method is used to measure the iodine value. The higher the iodine value, the higher the level of unsaturation in the oil. The iodine value of soybean oil was 126.41 g I₂/100g. After the epoxidation reaction, the measured iodine value was 3.33 % which suggests that the double bond in soybean oil became more reactive and can be further used.

3.1.2. Epoxy value

The epoxy value indicates the presence of the amount of epoxy group in the epoxide material. In this work, the epoxy oxygen content (EOC %) of ESBO after the synthesis from SBO was achieved at 6.6 %. After the carbonation reaction for 48 hr, the epoxy value for CSBO was recorded to be 0.2 % which confirms the successful conversion of the epoxy ring into cyclic polycarbonate.

3.1.3. Fourier-transform infrared spectroscopy

FTIR was utilized to determine the presence of various functional groups in the material using an infrared absorption spectrum. This technique was used to obtain the spectrum data of synthesized materials at ambient temperature to assess structural changes. These changes were identified through the shifting or disappearance of absorption peaks in the spectra. **Figure 13** depicts the FTIR spectra of SBO, ESBO, CSBO, and NIPU. The characteristic peak at 3011 cm^{-1} shows the ($=\text{C-H}$) hydrogen stretching from an unsaturated carbon in SBO spectra, and it is generally observed in some vegetable oils and fats in the range of $2989\text{--}3029\text{ cm}^{-1}$. During the epoxidation process, a notable change was observed in the ESBO spectrum. Specifically, the peak at approximately 3011 cm^{-1} , which is associated with the H-C= bond, was no longer present. However, a small peak appeared at 825 cm^{-1} , indicating the presence of a C-O-C ring which indicates that the reaction occurred between hydrogen peroxide and acetic acid. Furthermore, all spectra showed a peak at around 1700 cm^{-1} which was assigned to the C=O absorption from an ester bond. In the instance of CSBO, it was observed that apart from the absorption of the C=O bond in an ester at around 1700 cm^{-1} , there was an additional peak observed at around 1802 cm^{-1} , which may be attributed to the carbonate carbonyl. Along with this, the peak at 825 cm^{-1} disappeared in CSBO suggesting the presence of the cyclic carbonate structure indicating the conversion of the epoxy groups into cyclic carbonate [1][35][36].

Additionally, in the NIPU spectrum, the absorbance peak at 1802 cm^{-1} was absent and a broad band appeared within the range of 3200 cm^{-1} and 3500 cm^{-1} which could be attributed to the stretching vibration of N-H and O-H groups which are generally observed

around 3300 cm^{-1} and 3440 cm^{-1} the carbonate reacted with the amine group from EDA to form the hydroxy urethane [1].

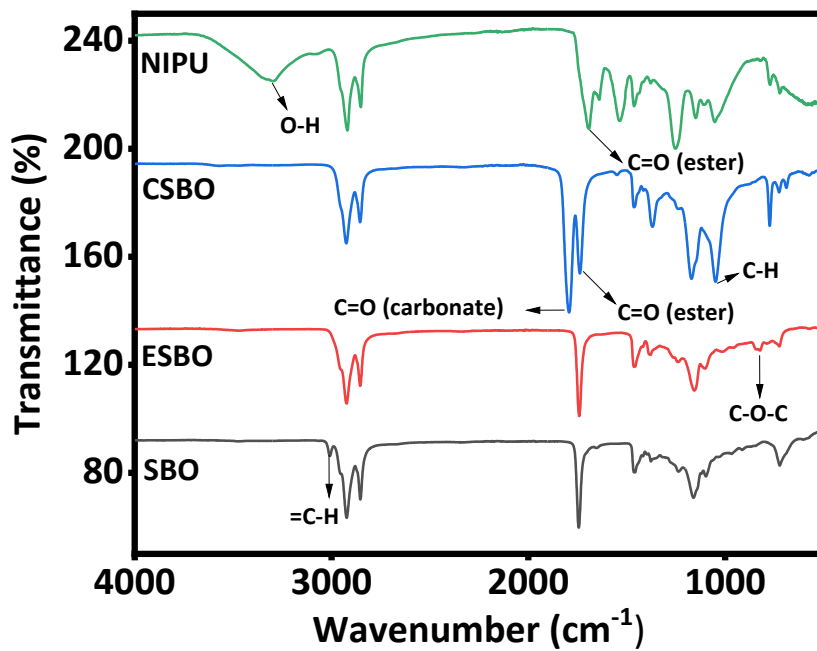


Figure 13: FTIR analysis of SBO, ESBO, CSBO, and NIPU.

3.1.4. Gel permeation chromatography

In GPC, the determination of the retention time is an important component since it serves to track the reaction process. Based on that, GPC was performed on SBO, ESBO, and CSBO as illustrated in **Figure 14**. It can be seen that SBO provided the highest retention time, which was around 23.39 minutes, indicating its lowest molecular weight compared to other components. It was expected that ESBO would have a slightly shorter retention time of 23.31 min because epoxidation involves adding a single oxygen atom to break up the double bonds, which leads to a relatively small rise in molecular weight. In

addition, CSBO had the shortest retention time at 22.70 minutes, resulting in the highest molecular weight. After undergoing the epoxidation and carbonation processes, the molecular weight of SBO increased, indicating the synthesis was successful.

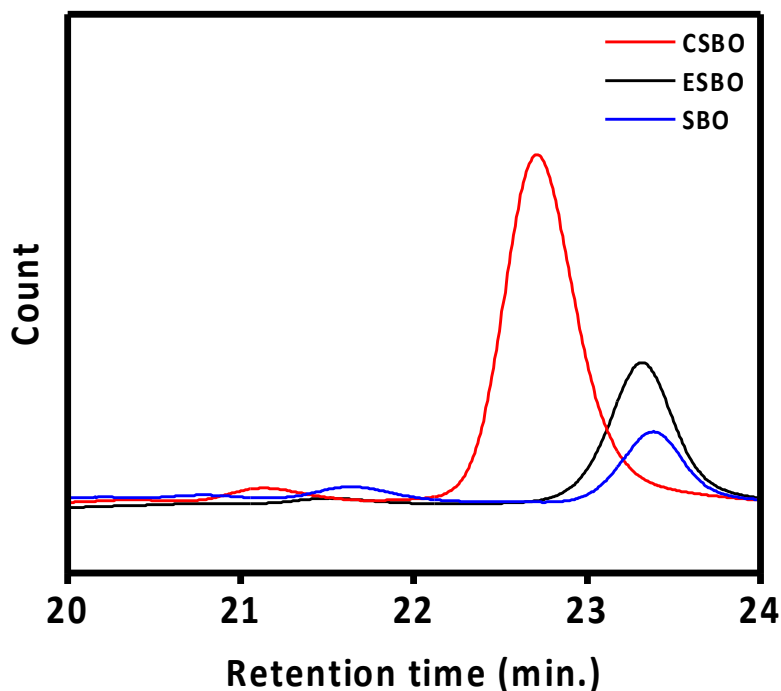


Figure 14: GPC analysis of SBO, ESBO, and CSBO.

3.1.5. Viscosity

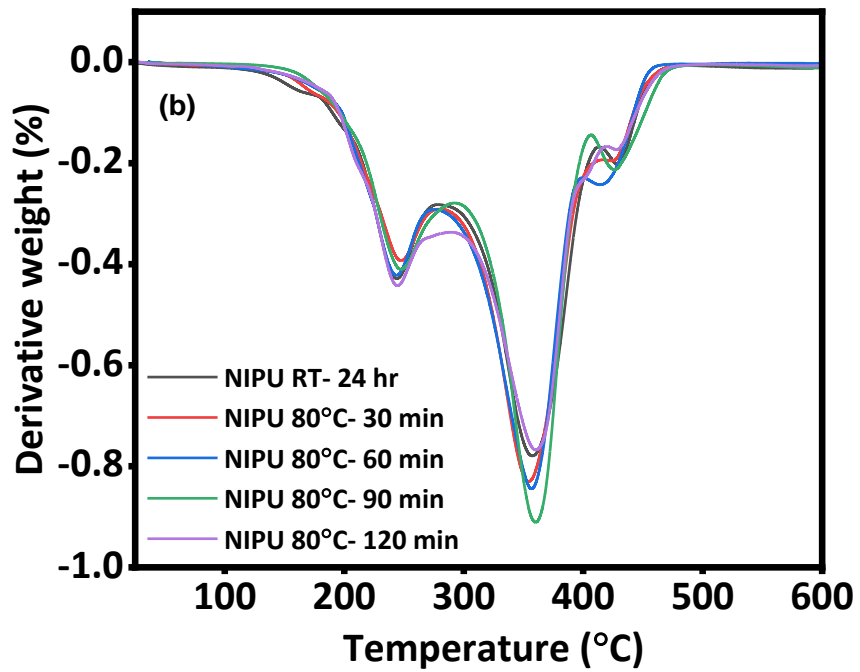
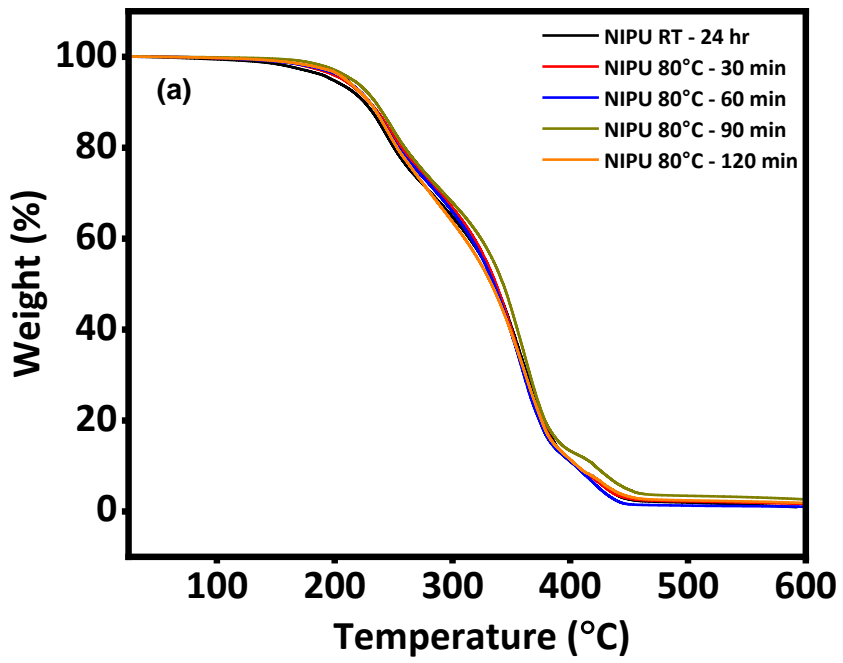
Viscosity is one of the most useful methods to determine the monitoring of a reaction. It was measured for the confirmation of an increase in molecular weight, which led to the successful conversion of ESBO from soybean oil and then ESBO to CSBO. Of the three different materials, SBO had the lowest viscosity at 0.19 Pa.s. The viscosity of the ESBO increased to 0.34 Pa.s as a result of the epoxidation procedure. After the carbonation process was complete, the CSBO that was formed had a viscosity that was significantly

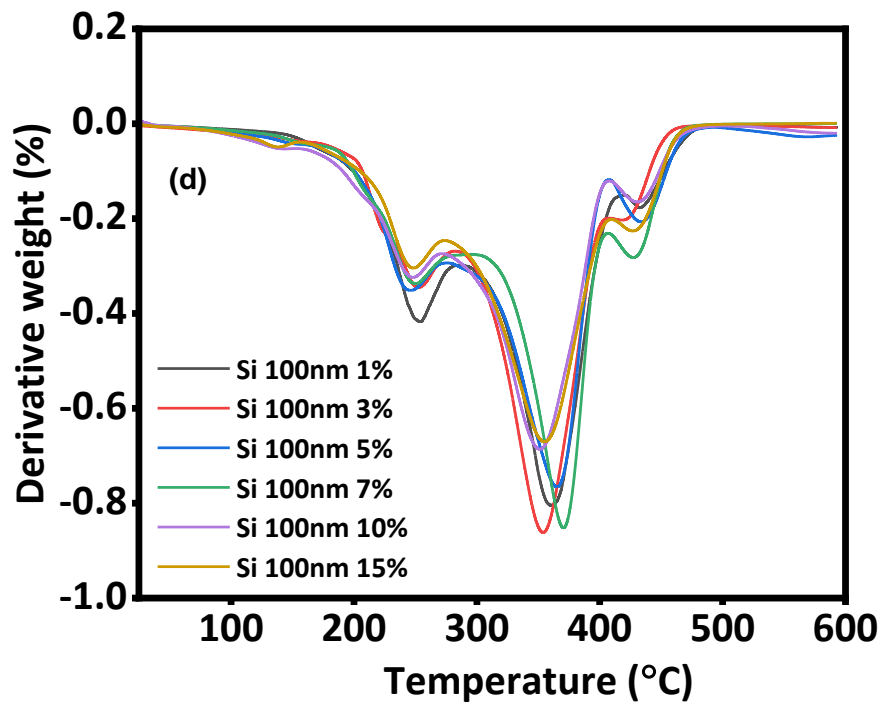
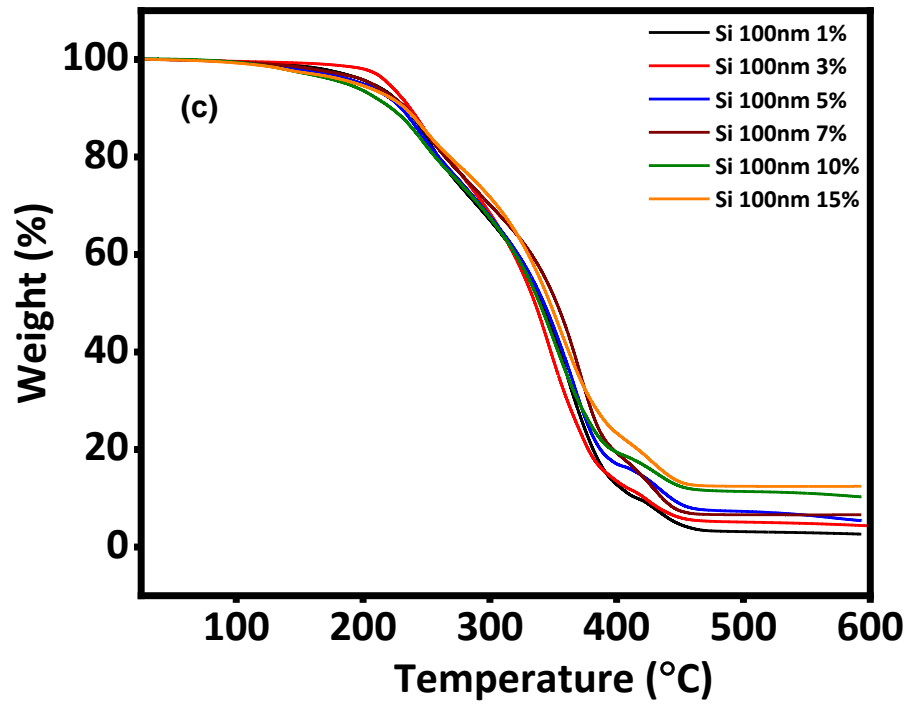
increased to 130 Pa.s. The significant rise could be explained by the more polarized bonds that result from the presence of carbonate groups, which are known to be capable of inducing a greater dipole-dipole interaction between molecules. Additionally, there is a possibility that an increase in viscosity could be linked to the significant rise in molecular weight that was observed by the use of GPC. This type of rheological behavior was seen in a prior investigation by Tamami *et al* [37].

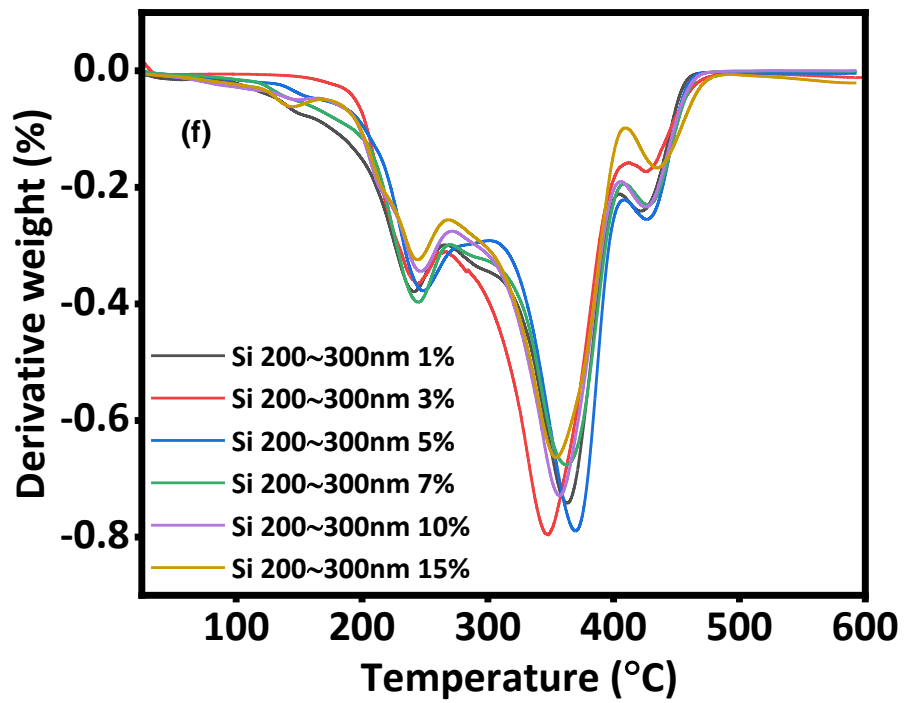
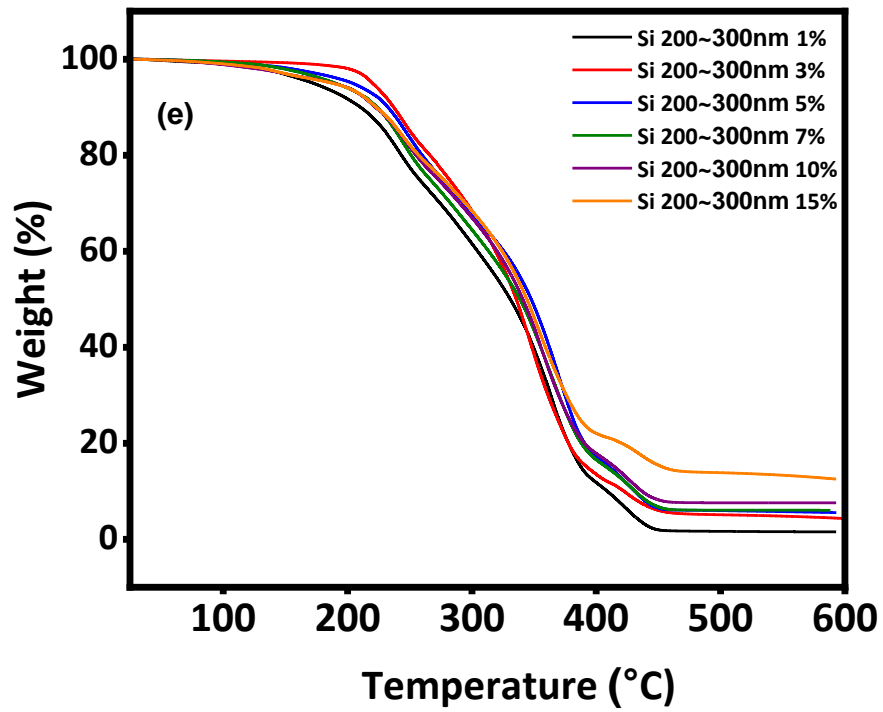
3.2. TGA

The thermal stability of the NIPU with and without nanofillers was characterized by TGA and DTGA results, which are shown in **Figure 15**. In all the NIPU adhesive samples, similar degradation behaviors were observed as the temperature increased. The initial degradation temperature of NIPU adhesives was recorded at above 235°C, which demonstrates outstanding thermal stability [38]. There was a three-step degradation observed for NIPU samples, which can be derived from the DTGA. All the samples shown in **Fig. 15(a)** and **2(b)** were cured at 80° C with variations in time to identify the thermal degradation. Three particle sizes of Si nanofiller were introduced to observe the thermal and mechanical stability of the NIPU adhesive. Figures (c), (d), (e), (f), (g), and (h) depict the TGA and DTGA graphs for Si 100 nm, 200-300 nm, and 500 nm, correspondingly. The initial degradation step was observed within the temperature range of 238–252 °C. The cause of this phenomenon can be attributed to the breakdown of the urethane bonds into carbon dioxide, alcohols, primary amines, and secondary amines. Moreover, the second and fastest degradation of NIPU adhesives was observed in the second stage, where the temperature was recorded in the range of 340–369 °C, which relates to the degradation of

the unsaturated fatty acid chains present in the CSBO [38]. The last thermal degradation stage witnessed above 415 °C might be attributed to the breakdown of residual components [38]. At 5% and 15% weight loss in all of the samples, it was noticed that the sample with Si 100 nm 3% demonstrated the maximum thermal stability at 220 °C and 250 °C, respectively, whereas the thermal stability of the control sample was measured at 214 °C which is shown in **Table 1**. The results of 5% and 15% weight loss were irregular in all particle sizes but it can be said that increasing particle size in NIPU leads to a decrease in thermal stability. Nevertheless, the results were not significant and showed minor changes. Furthermore, the weight (%) of residue remained at 590 °C for the control sample was 2.74% and by incorporating Si nanofillers, the results were increased by 11.62% for the sample with Si 500 nm 15 wt.%. In terms of residue remaining, the effect of nanofillers had a noteworthy impact on NIPU adhesive. According to the results of the TGA investigation, the presence of Si nanofillers did not have a significant impact on the thermal degradation behavior.







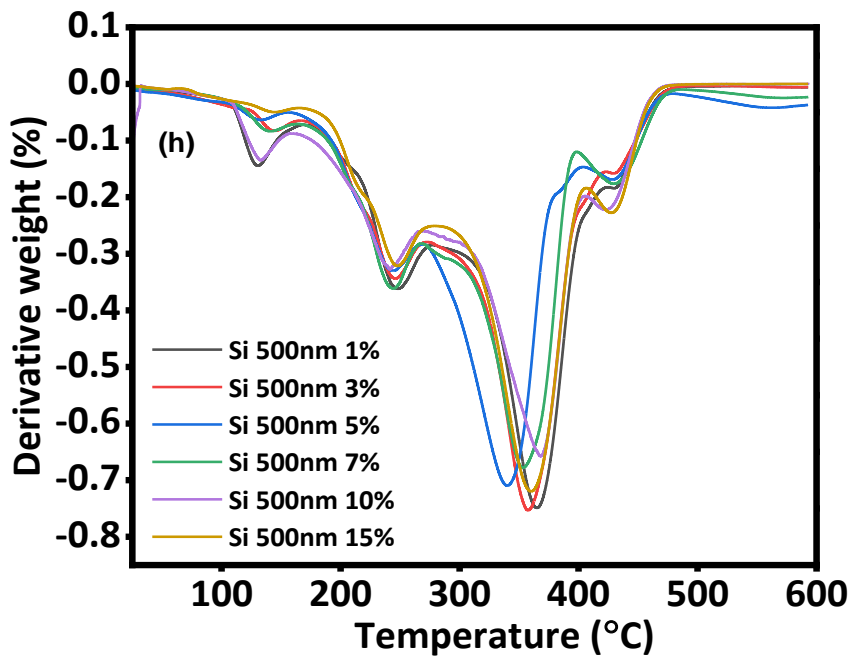
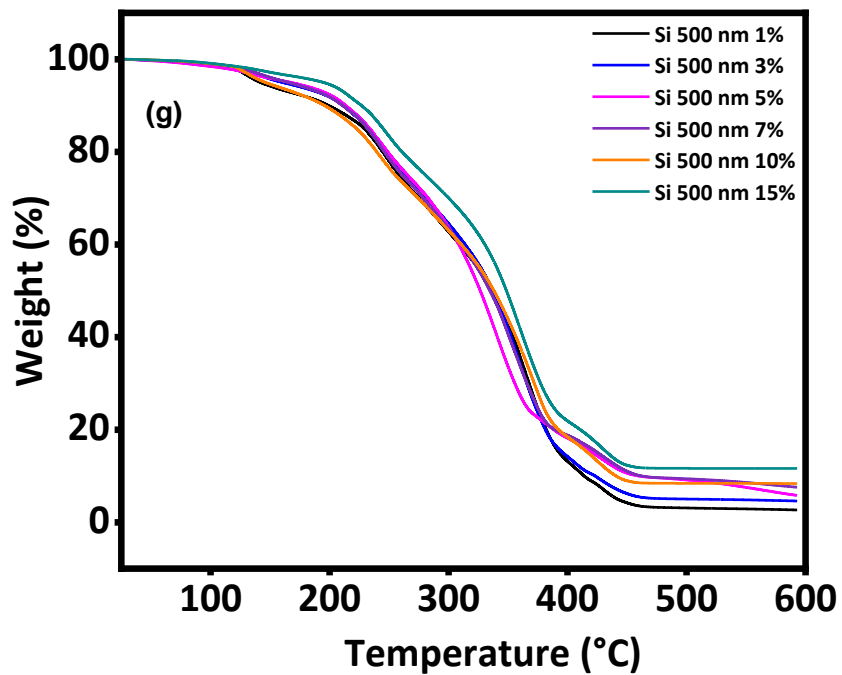


Figure 15: TGA analysis results

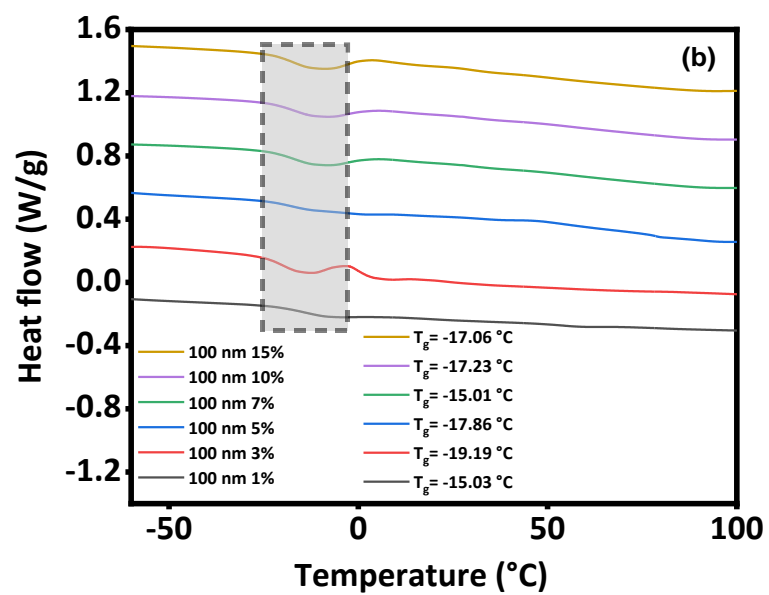
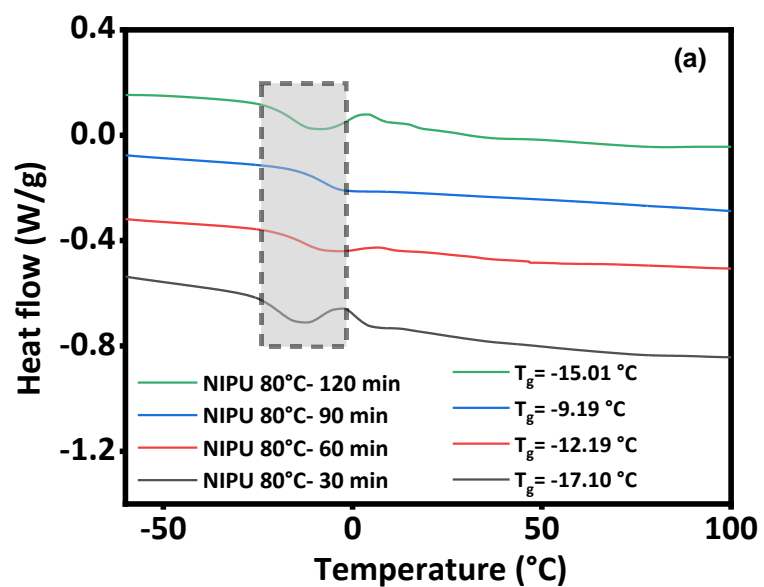
Table 1: TGA data for weight loss

Sample name	Temp. (°C) at 5% weight loss	Temp. (°C) at 15% weight loss	Weight (%) of residue remained at 590°C
NIPU/CNT STD	215	247	2.74
NIPU/100nm/3	220	250	4.43
NIPU/200~300nm/3	220	250	4.43
NIPU/500nm/15	194	245	11.62

3.3. DSC

The thermal transition behavior was observed with the help of DSC. The glass transition temperature (T_g) of all samples is shown in **Figure 16**. It was observed that the adhesives exhibited typical behavior characteristic of an amorphous material. This

behavior was attributed to the presence of a single endothermic thermal transition, which corresponded to the T_g . The T_g of the samples containing nanofillers is observed to range from -19.19 to -3.95°C, while the control sample exhibits a glass transition temperature of -9.19°C. Multiple factors can contribute to the achievement of a low T_g . These factors include intermolecular interactions, cross-linking density [39], moisture content, and the incorporation of fillers [40]. Another reason behind low T_g could be the flexibility of a material. Generally, flexible materials exhibit low T_g while brittle materials show high T_g . The inclusion of EDA in the NIPU can result in reduced intermolecular interactions among the polymer chains, thereby generating additional free volume. This increased free volume facilitates the movement of the polymer chains at lower temperatures, ultimately resulting in a lower T_g . Furthermore, the incorporation of nanofillers enhances the available free volume, thereby facilitating unrestricted movement. The relationship between free volume and glass transition temperature suggests that an increase in free volume corresponds to a decrease in the glass transition temperature. The DSC analysis revealed a significant impact of nanofillers on NIPU.



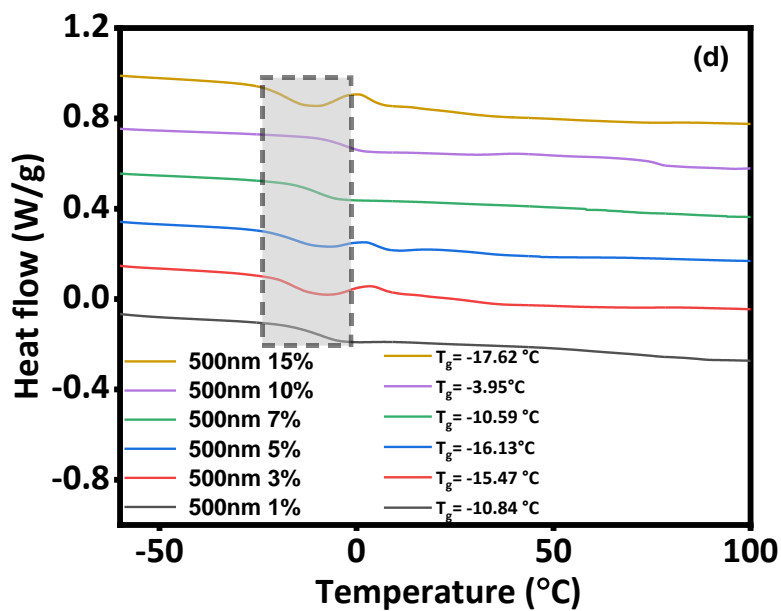
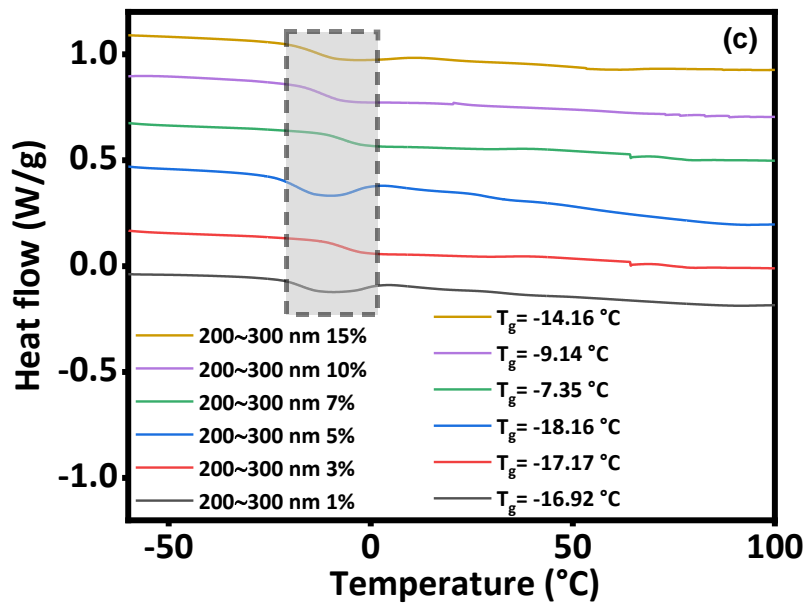


Figure 16: DSC plot of samples with (a) Variation in curing time (b) Si 100 nm (c) Si 200-300 nm (d) Si 500 nm

3.4. Contact angle measurement

Figure 17 shows the water contact angle studies of the surface morphology of the NIPU. The NIPU adhesive was coated smoothly on the wood specimen to identify its hydrophobic nature. The contact angle for the control sample was recorded at 97.60° , which reveals the hydrophobic behavior of the adhesive. After the introduction of Si nanofillers, an increase in the contact angle was observed. The highest contact was noticed at 131.8° with 7% (wt.% of CSBO) Si 200-300 nm. The observed phenomenon can be attributed to the rise in cross-linking density, resulting in an elevated surface roughness. This increased roughness allows the material to hold onto water droplets for an extended duration, exhibiting remarkable hydrophobic properties. The second highest contact angle was noticed at 3% (wt.% of CSBO) Si 100 nm, which showed 128.8° . In addition, the lowest result for Si 500 nm nanofiller was observed at 115.5° with 10% (wt.% of CSBO). Once a specific level of surface roughness is achieved, the intermolecular bonds cause the polymeric chains to come closer together, resulting in a reduction in hydrophobic properties.

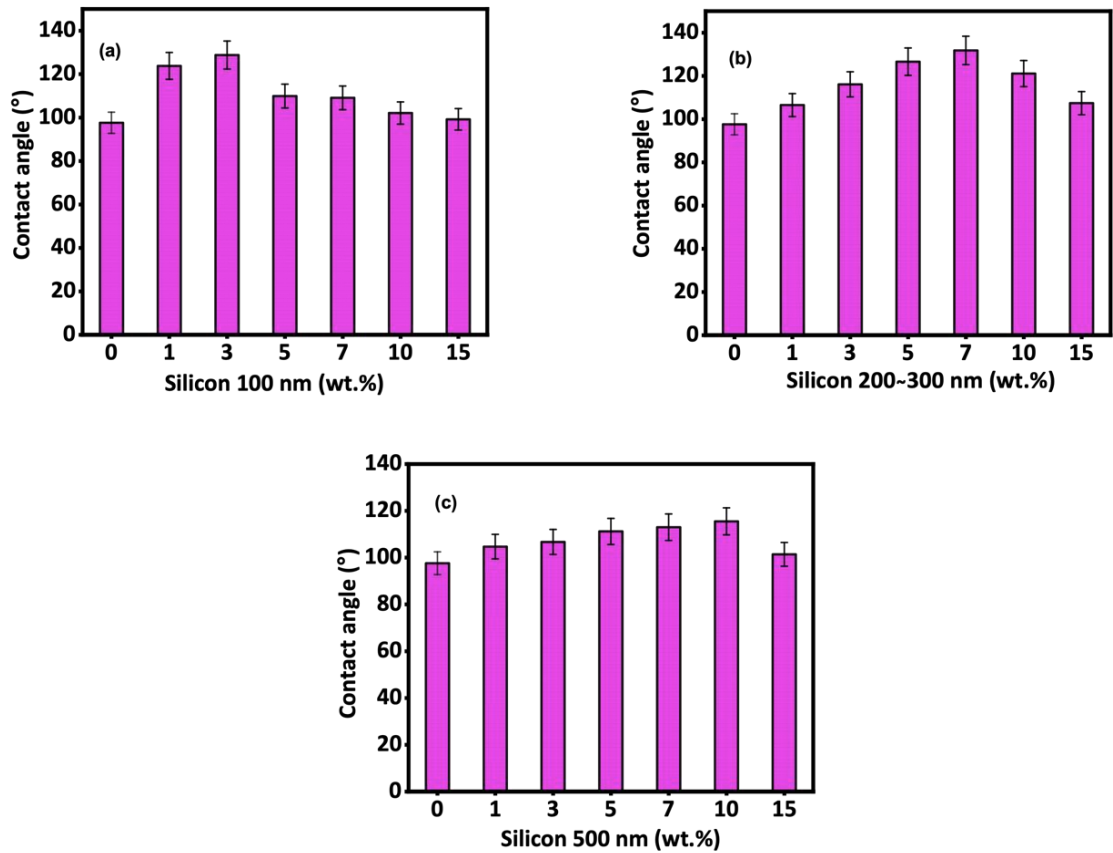


Figure 17: Contact angle of the control sample, Si 100, 200~300, and 500 nm nanofillers samples.

3.5. Single-lap shear strength

When it comes to adhesive, shear strength is the most significant test performed for the application in wood. To determine the bonding strength of the substrate, NIPU adhesive was applied to the oak wood substrate. The dimension of oak wood for the preparation of the specimen is shown in **Figure 18**. Approximately 140 g/m^2 was applied to the wood specimen. All the samples were cured in the oven with manual clamping curing technique as shown in **Figure 19**. An average of three samples were considered. Based on various types of failures obtained in wood specimens, the locus of failure was determined by

manual observation, as shown in **Table 2**. It was noticed that most of the samples showed substrate failure which can be seen in **Figure 21**. The equation utilized for the determination of the tensile shear strength is as follows: F_{max} represents the maximum force applied (N), A indicates the surface area of the adherend (mm^2) while a and b respectively refer to the width and length of the adherend (mm).

$$\text{Tensile shear strength (MPa)} = F_{max} / A = F_{max} / a \times b$$

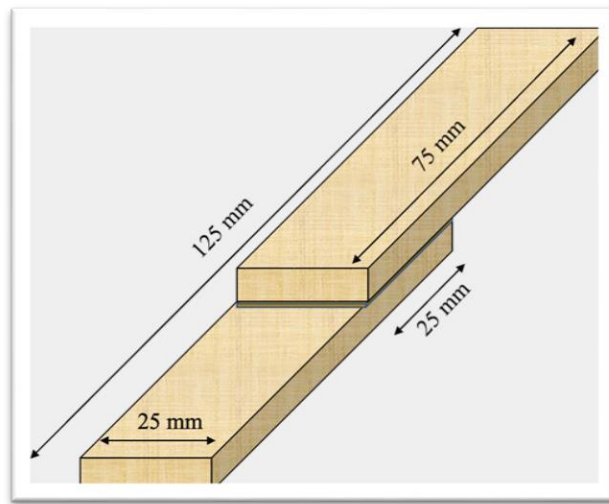


Figure 18: Dimensions of oak wood



Figure 19: Manual clamping method

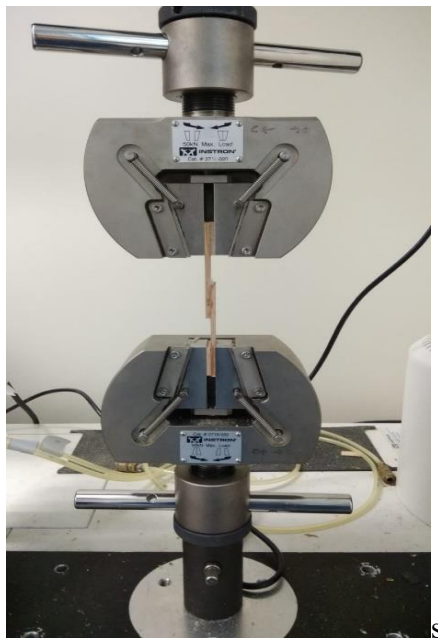


Figure 20: Tensile test performed on Instron M 3367



Figure 21: Substrate failure observed in specimens

3.5.1. Control sample

To obtain the best results with control samples, variations in time (30, 60, 90, and 120 min, respectively) and temperature (60, 80, 100, and 120°C, respectively) were performed without the addition of any fillers. The shear strength results are shown in **Figure 22**. The maximum strength of 8.81 MPa was observed in the samples that were cured at a temperature of 80°C for 90 minutes. This specific time and temperature were considered suitable for further testing with nanofillers.

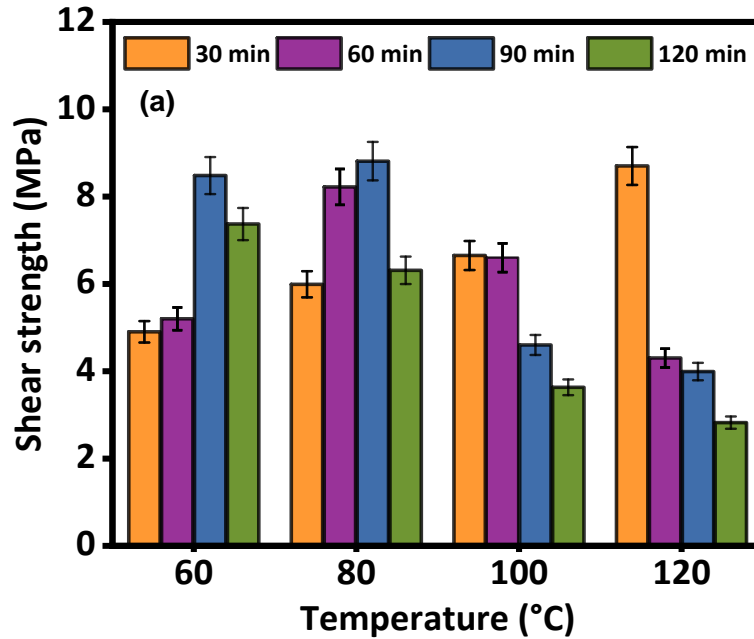


Figure 22: Shear strength with variation in curing times and temperatures

3.5.2. Effect of the Si nanofillers

After attaining incredible bonding strength with control samples by executing several changes in curing time and temperature, Si nanofillers with three particle sizes were incorporated to identify an improvement in tensile strength. Samples prepared with Si 100 nm nanofiller and cured with manual clamping technique, displayed an increasing trend in shear strength with increasing wt.% of Si 100 nm up to 7 wt.% which reached 9.85 MPa from 8.58 MPa in 1 wt.% samples as shown in **Figure 23**. The shear strength results for Si 100 nm were 8.58, 8.75, 9.34, 9.85, 8.71, and 6.65 MPa. 9.85 MPa was the best result achieved among all the samples. An overall increment of 10.56% was observed in comparison to the control sample. The reason behind the improvement of bonding strength after incorporating Si nanofillers could be related to the surface chemistry. Si nanoparticles shows high surface area because of their smaller particle size which gives more contact

points to interact with the adhesive and wood surface ultimately leads to an increase in shear strength.

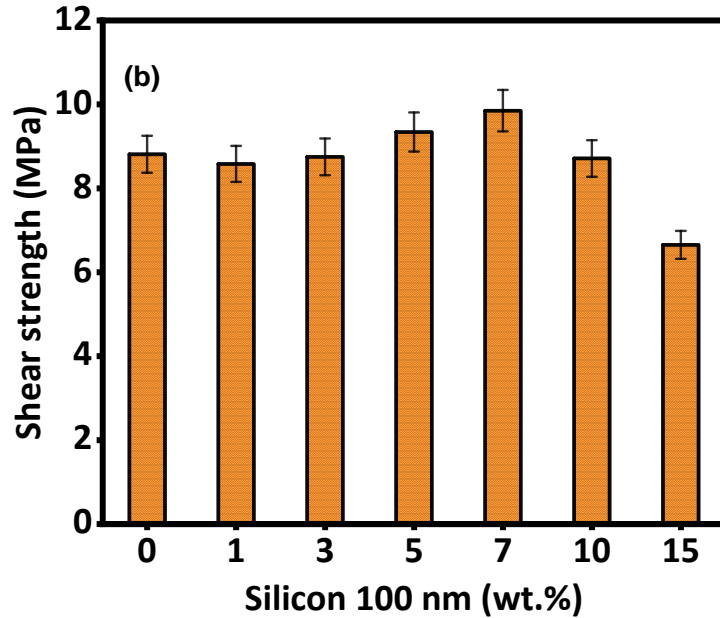


Figure 23: Shear strength of NIPU adhesive with Si 100 nm

The achieved shear strength in samples with Si 200-300 nm nanofillers for 1 wt.%, 3 wt.%, 5 wt.%, 10 wt.%, 15 wt.%, and 20 wt.% was 6.36 MPa, 7.04 MPa, 7.30 MPa, 7.32 MPa, 7.75 MPa, 9.62 MPa, and 6.64 MPa, respectively which can be seen in **Figure 24**. After 15 wt.%, a decrement in shear strength was recorded. An increment of 8.42% was obtained compared to the control sample. A similar trend was noticed after the addition of Si 500 nm nanofiller. It was noticed that after increasing the wt.% of Si 100 nm nanofiller, the shear strength also increased gradually to 10 wt.%. The results for samples with 1 wt.%, 3 wt.%, 5 wt.%, 7 wt.%, 10 wt.%, and 15 wt.% were 6.43 MPa, 6.87 MPa, 6.51 MPa, 6.87

MPa, 9.03 MPa, 8.65 MPa, respectively using Si 500 nm nanofillers as shown in **Figure 25**. In Si 500 nm, no significant improvement was observed except in the sample with 10 wt.%. An increment of 2.43% was obtained compared to the control sample. It can be seen from the results that after the addition of different particle sizes of Si nanofiller up to a specific wt.% in NIPU adhesive, the shear strength increased compared to control samples but decreased as the particle sizes of Si nanofiller (100 nm, 200-300 nm, and 500 nm, respectively) increased, which indicates that smaller particle size exhibits higher shear strength. The particle size has a significant impact on the mechanical properties of the NIPU adhesives. Furthermore, the reduction of particle size typically leads to an enhancement in surface area and enhanced dispersion within the adhesive layer. As a result, there is an increase in the bonding strength of the wood adhesive. Substrate failure (S.F) was observed in the majority of the samples, indicating the exceptional mechanical properties of the wood adhesive. Tensile strength results were very promising compared to some commercially available adhesives such as TitebondTM adhesive and WeldbondTM adhesive [41] and other research works as shown in **Table 3**.

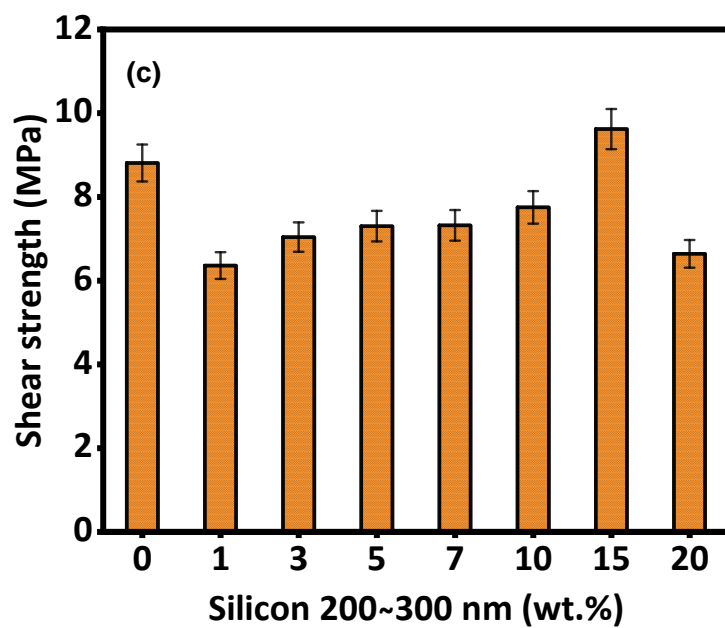


Figure 24: Shear strength of NIPU adhesive with Si 200-300 nm

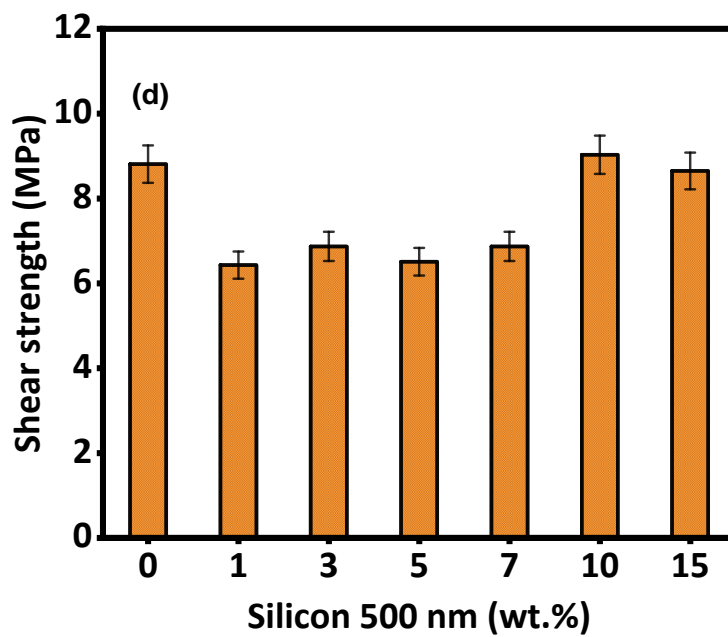


Figure 25: Shear strength of NIPU adhesive with Si 500 nm

Table 2: Locus of failure in NIPU adhesive

Sample name	Shear Strength (MPa)	Locus of failure (Substrate/Cohesive)
NIPU/100nm/1	8.58	S.F
NIPU/100nm/3	8.75	S.F
NIPU/100nm/5	9.34	S.F
NIPU/100nm/7	9.85	S.F
NIPU/100nm/10	8.71	S.F
NIPU/100nm/15	6.65	S.F
NIPU/Control	8.81	S.F

Sample name	Shear Strength (MPa)	Locus of failure (Substrate/Cohesive)
NIPU/200-300nm/1	6.36	C.F
NIPU/200-300nm/3	7.04	S.F
NIPU/200-300nm/5	7.30	S.F
NIPU/200-300nm/7	7.32	S.F
NIPU/200-300nm/10	7.75	S.F
NIPU/200-300nm/15	9.62	S.F
NIPU/200-300nm/20	6.64	C.F
NIPU/Control	8.81	S.F

Sample name	Shear Strength (MPa)	Locus of failure (Substrate/Cohesive)
NIPU/500nm/1	6.43	C.F
NIPU/500nm/3	6.87	S.F
NIPU/500nm/5	6.51	S.F
NIPU/500nm/7	6.87	S.F
NIPU/500nm/10	9.03	S.F
NIPU/500nm/15	8.65	S.F
NIPU/Control	8.81	S.F

Table 3: Comparison with other PU adhesives

Sample name	Lap shear strength (MPa)	References
Titebond™ adhesive	2.7	[41]
Weldbond™ adhesive	2.6	[41]
Lignin-based NIPU adhesive	0.77	[42]
SiO ₂ /Starch-based adhesive	5.12	[30]
Palm oil-based adhesive	5.3	[41]
Castor oil-based adhesive	2.19	[43]
Soy oil-based NIPU adhesive	9.85	Our work
Sucrose-based NIPU adhesive	1.02	[44]
Canola oil-based adhesive	5.7	[39]

CHAPTER IV

CONCLUSION

In the present research, bio-based polyurethane wood adhesives with the usage of soybean oil were successfully developed by employing a non-isocyanate approach which indicates a suitable alternative to petrochemical-based adhesives. An epoxidation reaction followed by a carbonation process was performed to produce CSBO. To determine the existence of CSBO and PU, a series of confirmatory tests were performed, including FT-IR analysis, iodine value, epoxy value, GPC analysis, and viscosity measurement. Furthermore, to prepare control samples, EDA was added into CSBO in a 1:1 molar ratio. Along with that, Si nanofillers were incorporated with variations in particle size (100, 200-300, and 500 nm) to notice the effect on mechanical and thermal properties. The combination of NIPU adhesives derived from renewable soybean oil and nanofillers has the potential to significantly increase the mechanical strength of wood adhesives. 9.85 MPa was the highest shear strength achieved among all the samples. It was observed that along with bonding strength, the hydrophobicity of the samples also decreased with an increase in nanofiller particle size which indicates a significant contribution of fillers. NIPU adhesives exhibit good thermal stability up to 230° C. NIPU coated samples also gave a contact angle at 131.8° which shows the excellent hydrophobic nature of the coated film,

indicating the incorporation of nanofillers into soy-based NIPU makes it suitable for utilization of wood adhesive showing outstanding mechanical properties.

CHAPTER V

FUTURE WORK

The current work might be broadened to investigate the effect of different cross-linkers and fillers or additives on the mechanical and thermal characteristics of non-isocyanate-based wood adhesives. Soybean oil-based adhesives can be compared to various vegetable oils-based wood adhesives. Furthermore, wet shear strength can be measured along with dry shear strength by preparing and placing samples under water for a specific period of time which is a significant aspect of wood applications under water. Bio-based amines can be used to reduce the toxicity in NIPU wood adhesives. Along with manual clamping, different curing techniques such as hot press can be applied to observe the effect on shear strength.

REFERENCES

- [1] I. Javni, D. P. Hong, and Z. S. Petrovič, “Polyurethanes from soybean oil, aromatic, and cycloaliphatic diamines by nonisocyanate route,” *Journal of Applied Polymer Science*, vol. 128, no. 1, pp. 566–571, Apr. 2013, doi: 10.1002/app.38215.
- [2] F. M. De Souza, M. R. Sulaiman, and R. K. Gupta, “Materials and Chemistry of Polyurethanes,” in *ACS Symposium Series*, vol. 1399, American Chemical Society, 2021, pp. 1–36. doi: 10.1021/bk-2021-1399.ch001.
- [3] A. Tenorio-Alfonso, M. C. Sánchez, and J. M. Franco, “A Review of the Sustainable Approaches in the Production of Bio-based Polyurethanes and Their Applications in the Adhesive Field,” *Journal of Polymers and the Environment*, vol. 28, no. 3. Springer, pp. 749–774, Mar. 01, 2020. doi: 10.1007/s10924-020-01659-1.
- [4] A. Cornille, R. Auvergne, O. Figovsky, B. Boutevin, and S. Caillol, “A perspective approach to sustainable routes for non-isocyanate polyurethanes,” *European Polymer Journal*, vol. 87. Elsevier Ltd, pp. 535–552, Feb. 01, 2017. doi: 10.1016/j.eurpolymj.2016.11.027.
- [5] L. Poussard *et al.*, “Non-Isocyanate Polyurethanes from Carbonated Soybean Oil Using Monomeric or Oligomeric Diamines to Achieve Thermosets or Thermoplastics,” *Macromolecules*, vol. 49, no. 6, pp. 2162–2171, Mar. 2016, doi: 10.1021/acs.macromol.5b02467.
- [6] C. Liang *et al.*, “Material Flows of Polyurethane in the United States,” *Environ Sci Technol*, vol. 55, no. 20, pp. 14215–14224, Oct. 2021, doi: 10.1021/acs.est.1c03654.
- [7] V. Suthar, M. A. Asare, F. M. de Souza, and R. K. Gupta, “Effect of Graphene Oxide and Reduced Graphene Oxide on the Properties of Sunflower Oil-Based Polyurethane Films,” *Polymers (Basel)*, vol. 14, no. 22, Nov. 2022, doi: 10.3390/polym14224974.
- [8] S. Gupta and R. Upadhyaya, “CANCER AND P21 PROTEIN EXPRESSION: IN RELATION WITH ISOCYANATE TOXICITY IN CULTURED MAMMALIAN CELLS,” *Swati Gupta, IJPRBS*, vol. 3, no. 6, pp. 20–28, 2014, [Online]. Available: www.ijprbs.com
- [9] D. Bello *et al.*, “Skin exposure to isocyanates: Reasons for concern,” *Environmental Health Perspectives*, vol. 115, no. 3. pp. 328–335, Mar. 2007. doi: 10.1289/ehp.9557.
- [10] S. Tan, T. Abraham, D. Ference, and C. W. MacOsco, “Rigid polyurethane foams from a soybean oil-based Polyol,” *Polymer (Guildf)*, vol. 52, no. 13, pp. 2840–2846, Jun. 2011, doi: 10.1016/j.polymer.2011.04.040.

- [11] S. Dworakowska, D. Bogdal, and A. Prociak, “Microwave-assisted synthesis of polyols from rapeseed oil and properties of flexible polyurethane foams,” *Polymers (Basel)*, vol. 4, no. 3, pp. 1462–1477, 2012, doi: 10.3390/polym4031462.
- [12] S. Ramanujam, C. Zequine, S. Bhoyate, B. Neria, P. Kahol, and R. Gupta, “Novel Biobased Polyol Using Corn Oil for Highly Flame-Retardant Polyurethane Foams,” *C (Basel)*, vol. 5, no. 1, p. 13, Mar. 2019, doi: 10.3390/c5010013.
- [13] M. A. Asare, P. Kote, S. Chaudhary, F. M. de Souza, and R. K. Gupta, “Sunflower Oil as a Renewable Resource for Polyurethane Foams: Effects of Flame-Retardants,” *Polymers (Basel)*, vol. 14, no. 23, Dec. 2022, doi: 10.3390/polym14235282.
- [14] Z. S. Petrović, W. Zhang, and I. Javni, “Structure and properties of polyurethanes prepared from triglyceride polyols by ozonolysis,” *Biomacromolecules*, vol. 6, no. 2, pp. 713–719, Mar. 2005, doi: 10.1021/bm049451s.
- [15] P. Alagi *et al.*, “Functional soybean oil-based polyols as sustainable feedstocks for polyurethane coatings,” *Ind Crops Prod*, vol. 113, pp. 249–258, Mar. 2018, doi: 10.1016/j.indcrop.2018.01.041.
- [16] F. M. de Souza, J. Choi, S. Bhoyate, P. K. Kahol, and R. K. Gupta, “Expendable Graphite as an Efficient Flame-Retardant for Novel Partial Bio-Based Rigid Polyurethane Foams,” *C — Journal of Carbon Research*, vol. 6, no. 2, p. 27, May 2020, doi: 10.3390/c6020027.
- [17] Y. Li, X. Luo, and S. Hu, “SPRINGER BRIEFS IN MOLECULAR SCIENCE GREEN CHEMISTRY FOR SUSTAINABILITY Bio-based Polyols and Polyurethanes.” [Online]. Available: <http://www.springer.com/series/10045>
- [18] A. Das and P. Mahanwar, “A brief discussion on advances in polyurethane applications,” *Advanced Industrial and Engineering Polymer Research*, vol. 3, no. 3. KeAi Communications Co., pp. 93–101, Jul. 01, 2020. doi: 10.1016/j.aiepr.2020.07.002.
- [19] J. O. Akindoyo, M. D. H. Beg, S. Ghazali, M. R. Islam, N. Jeyaratnam, and A. R. Yuvaraj, “Polyurethane types, synthesis and applications-a review,” *RSC Advances*, vol. 6, no. 115. Royal Society of Chemistry, pp. 114453–114482, 2016. doi: 10.1039/c6ra14525f.
- [20] P. Cinelli, I. Anguillesi, and A. Lazzeri, “Green synthesis of flexible polyurethane foams from liquefied lignin,” in *European Polymer Journal*, Jun. 2013, pp. 1174–1184. doi: 10.1016/j.eurpolymj.2013.04.005.
- [21] A. S. More, T. Lebarbé, L. Maisonneuve, B. Gadenne, C. Alfos, and H. Cramail, “Novel fatty acid based di-isocyanates towards the synthesis of thermoplastic polyurethanes,” *European Polymer Journal*, vol. 49, no. 4, pp. 823–833, Apr. 2013, doi: 10.1016/j.eurpolymj.2012.12.013.

- [22] O. Jaudouin *et al.*, “Ionomer-based polyurethanes: a comparative study of properties and applications Ionomer-based polyurethanes: a comparative study of properties and applications. Polymer inter-national Ionomer-based polyurethanes: a comparative study of properties and applications,” Society of Chemical Industry, vol. 61, no. 4, 2012, doi: 10.1002/pi.4156i.
- [23] L. Rocha, B. Dourado, L. A. Fonseca Pascoal, N. K. Sakomura, F. Guilherme Perazzo Costa, and D. Biagiotti, “8 Soybeans (Glycine max) and Soybean Products in Poultry and Swine Nutrition.” [Online]. Available: www.intechopen.com
- [24] Y. Li, E. Griffing, M. Higgins, and M. Overcash, “LIFE CYCLE ASSESSMENT OF SOYBEAN OIL PRODUCTION,” 2006.
- [25] R. C. PETERSEN, “The Chemical Composition of Wood,” 1984, pp. 57–126. doi: 10.1021/ba-1984-0207.ch002.
- [26] S. J. Marshall, S. C. Bayne, R. Baier, A. P. Tomsia, and G. W. Marshall, “A review of adhesion science,” *Dental Materials*, vol. 26, no. 2, 2010, doi: 10.1016/j.dental.2009.11.157.
- [27] A. V. Pocius, “Adhesion and Adhesives Technology,” in *Adhesion and Adhesives Technology*, Carl Hanser Verlag GmbH & Co. KG, 2012, pp. I–XVI. doi: 10.3139/9783446431775.fm.
- [28] “Adhesive properties Intro ref”.
- [29] “Intro ref 29”.
- [30] Z. Wang, Z. Gu, Y. Hong, L. Cheng, and Z. Li, “Bonding strength and water resistance of starch-based wood adhesive improved by silica nanoparticles,” *Carbohydrate Polymers*, vol. 86, no. 1, pp. 72–76, Aug. 2011, doi: 10.1016/j.carbpol.2011.04.003.
- [31] D. D. Plaza *et al.*, “Direct valorisation of waste cocoa butter triglycerides via catalytic epoxidation, ring-opening and polymerisation,” *Journal of Chemical Technology and Biotechnology*, vol. 92, no. 9, pp. 2254–2266, Sep. 2017, doi: 10.1002/jctb.5292.
- [32] V. J. Hattimattur, V. R. Sangale, P. S. Zade, M. B. Mandake, and S. Walke, “Review: Epoxidation of Vegetable oils.” [Online]. Available: www.ijtrd.com
- [33] I. Javni, D. P. Hong, and Z. S. Petrovič, “Polyurethanes from soybean oil, aromatic, and cycloaliphatic diamines by nonisocyanate route,” *Journal of Applied Polymer Science*, vol. 128, no. 1, pp. 566–571, Apr. 2013, doi: 10.1002/app.38215.
- [34] Neswati and N. Nazir, “Combination of temperature and time in epoxidation for producing epoxidized palm oil as source of bio polyol,” in *IOP Conference Series: Earth and Environmental Science*, IOP Publishing Ltd, May 2021. doi: 10.1088/1755-1315/757/1/012069.

- [35] M. Bähr, A. Bitto, and R. Mülhaupt, “Cyclic limonene dicarbonate as a new monomer for non-isocyanate oligo- and polyurethanes (NIPU) based upon terpenes,” *Green Chemistry*, vol. 14, no. 5, pp. 1447–1454, 2012, doi: 10.1039/c2gc35099h.
- [36] M. J. Lerma-García, G. Ramis-Ramos, J. M. Herrero-Martínez, and E. F. Simó-Alfonso, “Authentication of extra virgin olive oils by Fourier-transform infrared spectroscopy,” *Food Chem*, vol. 118, no. 1, pp. 78–83, Jan. 2010, doi: 10.1016/j.foodchem.2009.04.092.
- [37] B. Tamami, S. Sohn, and G. L. Wilkes, “Incorporation of Carbon Dioxide into Soybean Oil and Subsequent Preparation and Studies of Non isocyanate Polyurethane Networks,” *Journal of Applied Polymer Science*, 2004.
- [38] T. Wang *et al.*, “Mechanically strong non-isocyanate polyurethane thermosets from cyclic carbonate linseed oil,” *Green Chemistry*, vol. 24, no. 21, pp. 8355–8366, Sep. 2022, doi: 10.1039/d2gc02910c.
- [39] X. Kong, G. Liu, and J. M. Curtis, “Characterization of canola oil based polyurethane wood adhesives,” *International Journal for Adhesives and Adhesions*, vol. 31, no. 6, pp. 559–564, Sep. 2011, doi: 10.1016/j.ijadhadh.2011.05.004.
- [40] A. Farhadian, A. Ahmadi, I. Omrani, A. B. Miyardan, M. A. Varfolomeev, and M. R. Nabid, “Synthesis of fully bio-based and solvent free non-isocyanate poly (ester amide/urethane) networks with improved thermal stability on the basis of vegetable oils,” *Polymer Degradation and Stability*, vol. 155, pp. 111–121, Sep. 2018, doi: 10.1016/j.polymdegradstab.2018.07.010.
- [41] A. Khoon Poh, L. Choy Sin, C. Sit Foon, and C. Cheng Hock, “Polyurethane wood adhesive from palm oil-based polyester polyol,” *J Adhes Sci Technol*, vol. 28, no. 11, pp. 1020–1033, Jun. 2014, doi: 10.1080/01694243.2014.883772.
- [42] J. Saražin, A. Pizzi, S. Amirou, D. Schmiedl, and M. Šernek, “Organosolv lignin for non-isocyanate based polyurethanes (Nipu) as wood adhesive,” *J Renew Mater*, vol. 9, no. 5, pp. 881–907, 2021, doi: 10.32604/jrm.2021.015047.
- [43] B. B. R. Silva, R. M. C. Santana, and M. M. C. Forte, “A solventless castor oil-based PU adhesive for wood and foam substrates,” *International Journal for Adhesives and Adhesions*, vol. 30, no. 7, pp. 559–565, Oct. 2010, doi: 10.1016/j.ijadhadh.2010.07.001.
- [44] X. Xi *et al.*, “Non-isocyanate polyurethane adhesive from sucrose used for particleboard,” *Wood Sci Technol*, vol. 53, no. 2, pp. 393–405, Mar. 2019, doi: 10.1007/s00226-019-01083-2.